

Supporting information for:

Solution Structure, Electronic Energy Levels, and Photophysical Properties of $[\text{Eu}(\text{MeOH})_{n-2m}(\text{NO}_3)_m]^{3-m+}$ complexes

Nicolaj Kofod, Patrick Nawrocki, Mikkel Juels holt, Troels Lindahl Christiansen, Kirsten M. Ø. Jensen* and Thomas Just Sørensen*

Nano-Science Center & Department of Chemistry, University of Copenhagen, Universitetsparken 5, 2100 København Ø, Denmark

Contents

Supporting information for:	1
Optical Spectroscopy	2
Absorption, MeOH	3
Emission, MeOH	6
Lifetime traces	13
Absorption, MeOH-d ₄	17
Emission, MeOH-d ₄	20
Speciation Modelling	23
Dynafit Traces and Fits	23
Confidence interval profiles from Dynafit	30
Best Fit Parameters	31
Speciation plots	33
Photophysics	34
X-ray Total Scattering	37
Normalized G(r)	37
Normalized I(Q)	40
Models, Solid state based	43
Models, Geometrical	44

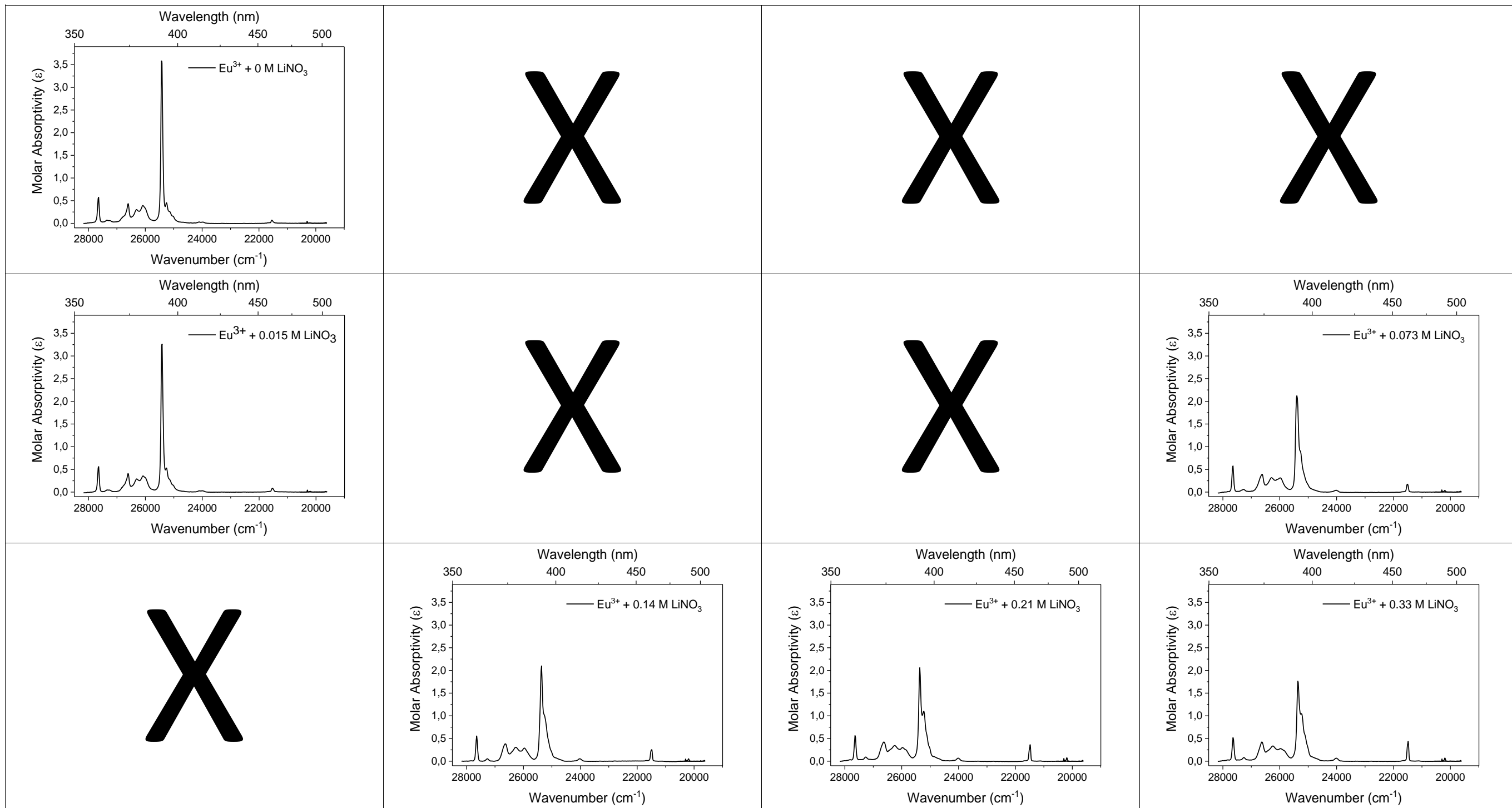
Data legend

The individual data from each sample is displayed in tables. In each dataset is displayed with the samples in the same position of the table. If a given data point is not recorded and X is displayed at the corresponding position.

0.1 M Eu(CF ₃ SO ₃) ₃ 0 M LiNO ₃	0.1 M Eu(CF ₃ SO ₃) ₃ 0.003 M LiNO ₃	0.1 M Eu(CF ₃ SO ₃) ₃ 0.006 M LiNO ₃	0.1 M Eu(CF ₃ SO ₃) ₃ 0.009 M LiNO ₃
0.1 M Eu(CF ₃ SO ₃) ₃ 0.015 M LiNO ₃	0.1 M Eu(CF ₃ SO ₃) ₃ 0.030 M LiNO ₃	0.1 M Eu(CF ₃ SO ₃) ₃ 0.059 M LiNO ₃	0.1 M Eu(CF ₃ SO ₃) ₃ 0.073 M LiNO ₃
0.1 M Eu(CF ₃ SO ₃) ₃ 0.10 M LiNO ₃	0.1 M Eu(CF ₃ SO ₃) ₃ 0.14 M LiNO ₃	0.1 M Eu(CF ₃ SO ₃) ₃ 0.21 M LiNO ₃	0.1 M Eu(CF ₃ SO ₃) ₃ 0.33 M LiNO ₃
0.1 M Eu(CF ₃ SO ₃) ₃ 0.50 M LiNO ₃	0.1 M Eu(CF ₃ SO ₃) ₃ 0.78 M LiNO ₃	0.1 M Eu(CF ₃ SO ₃) ₃ 1.00 M LiNO ₃	0.1 M Eu(CF ₃ SO ₃) ₃ 1.29 M LiNO ₃
0.1 M Eu(CF ₃ SO ₃) ₃ 1.50 M LiNO ₃	0.1 M Eu(CF ₃ SO ₃) ₃ 1.89 M LiNO ₃	0.1 M Eu(CF ₃ SO ₃) ₃ 2.00 M LiNO ₃	

Optical Spectroscopy

Absorption, MeOH



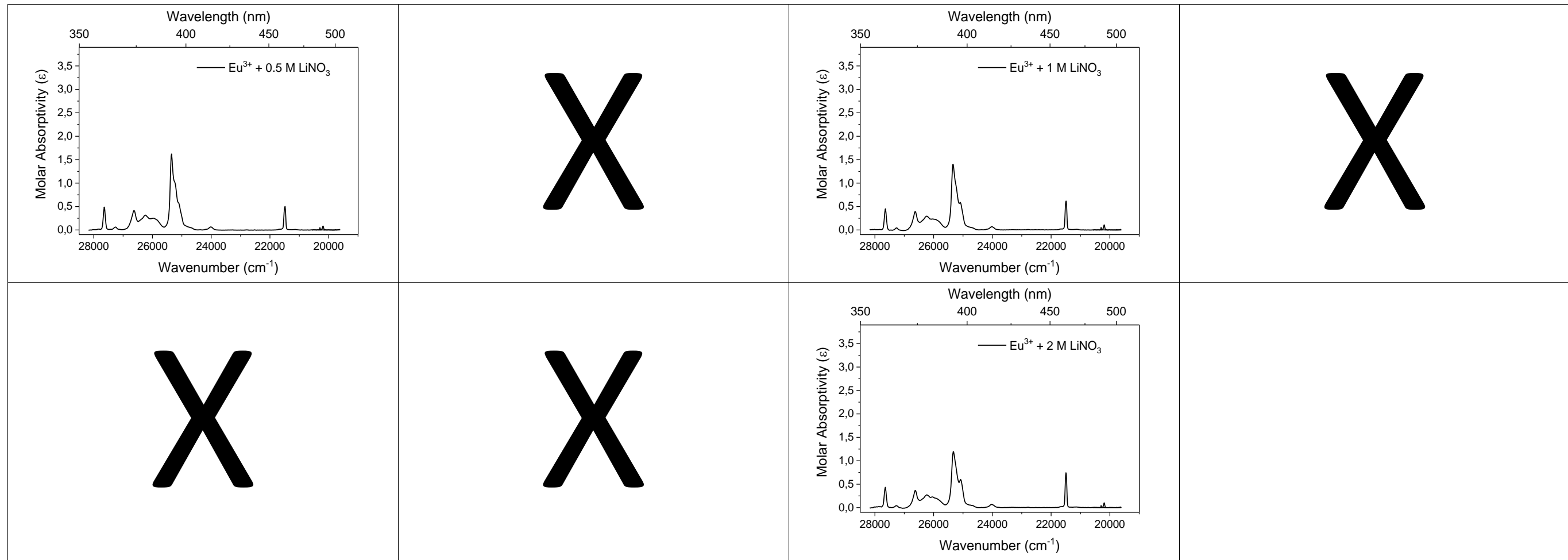


Figure S1: Absorption spectra of 0.1M $\text{Eu}(\text{CF}_3\text{SO}_3)_3$ in MeOH with concentrations of LiNO_3 from 0 to 2M at room temperature. Slits were kept at 1 nm.

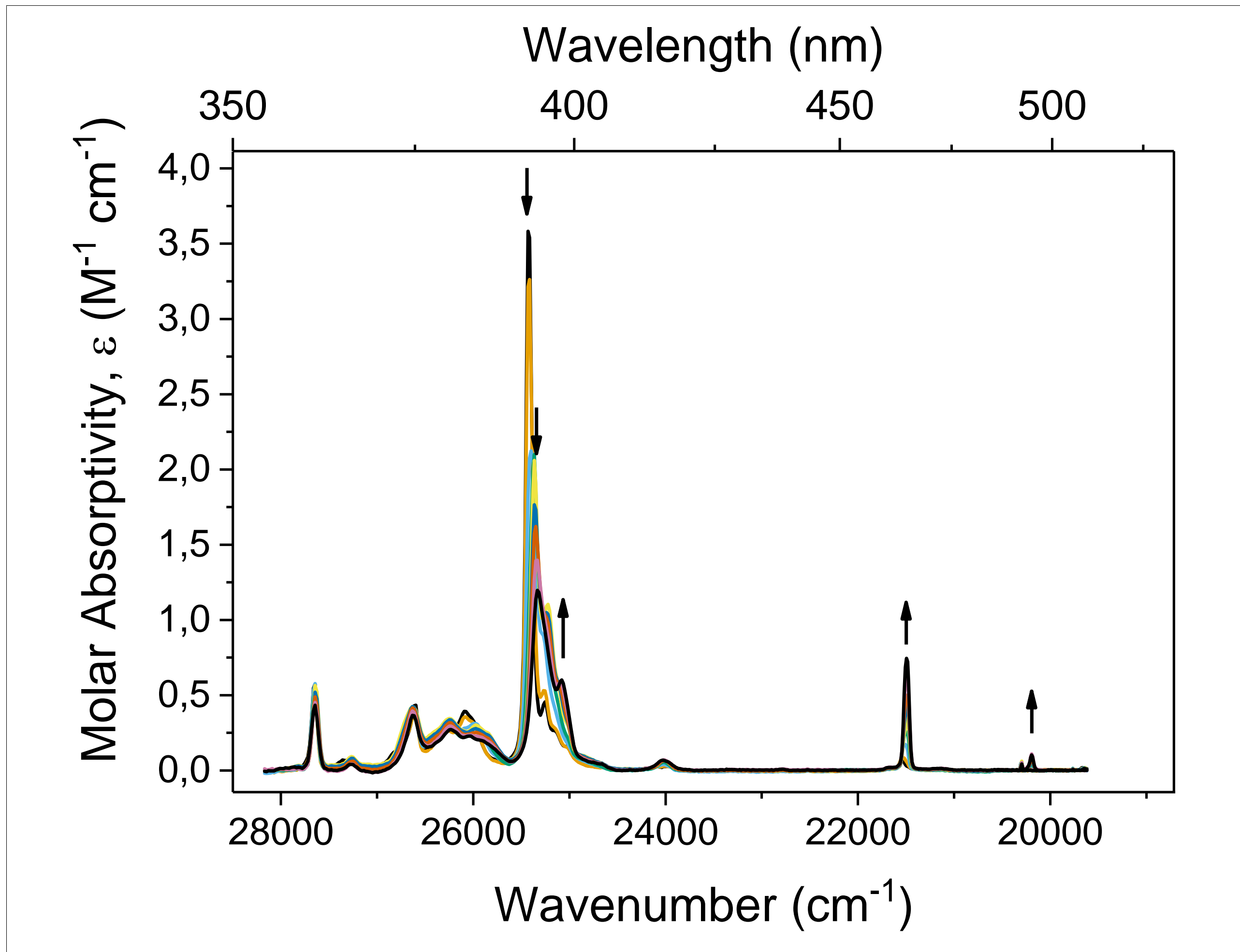
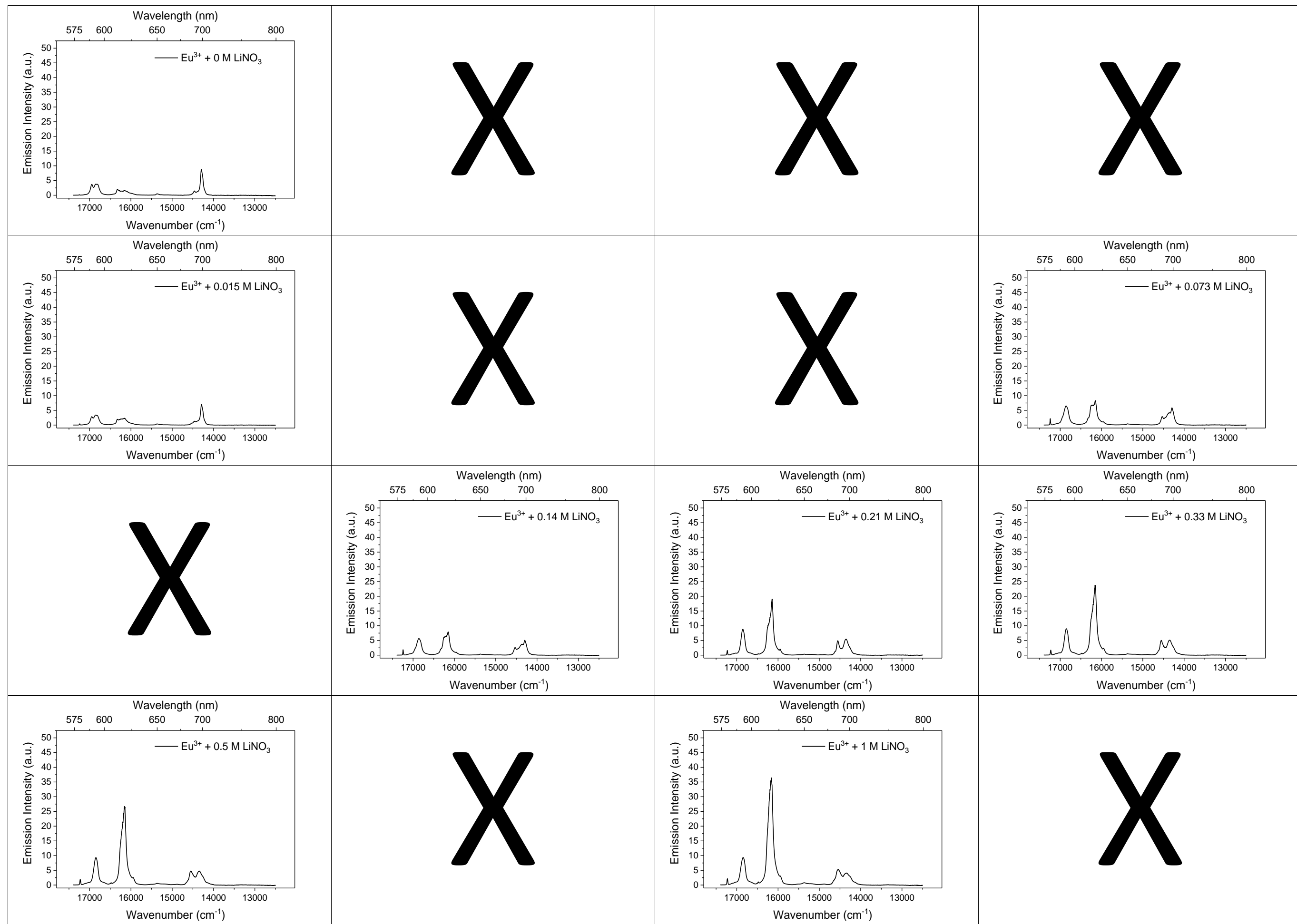


Figure S2: Absorption spectra of 0.1M $\text{Eu}(\text{CF}_3\text{SO}_3)_3$ in MeOH with concentrations of LiNO_3 from 0 to 2M at room temperature. Slits were kept at 1 nm. Arrows indicate changes in absorption as a function of increasing LiNO_3 .

Emission, MeOH

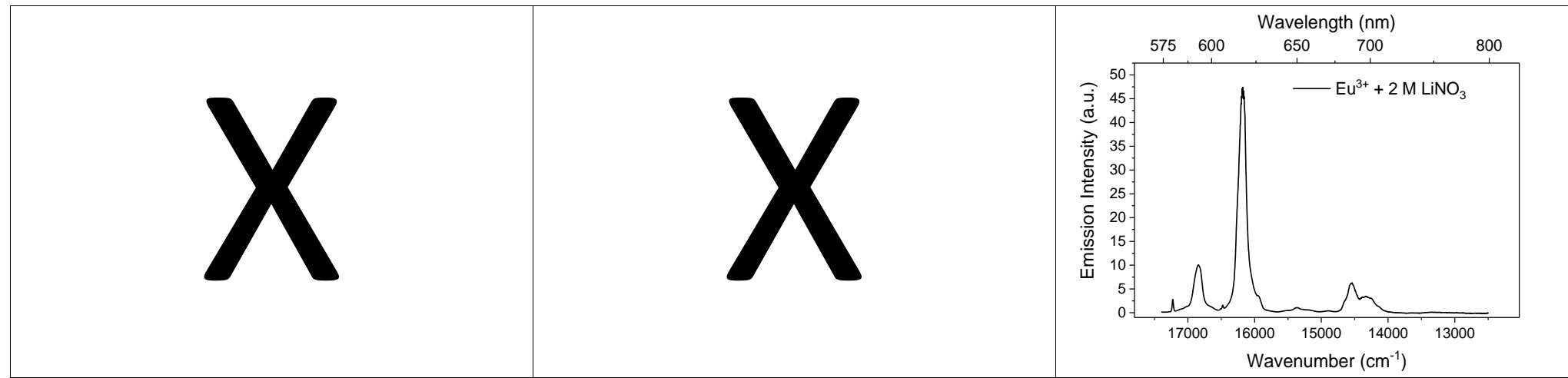


Figure S3: Emission spectra of 0.1M Eu(CF₃SO₃)₃ in MeOH with concentrations of LiNO₃ from 0 to 2M at 20 °C, excited at 394nm. Emission and excitation slits were kept at 0.4 and 8 nm respectively. Intensity was corrected for wavelength dependent detector sensibility and lamp intensity with a reference detector and factory supplied correction files.

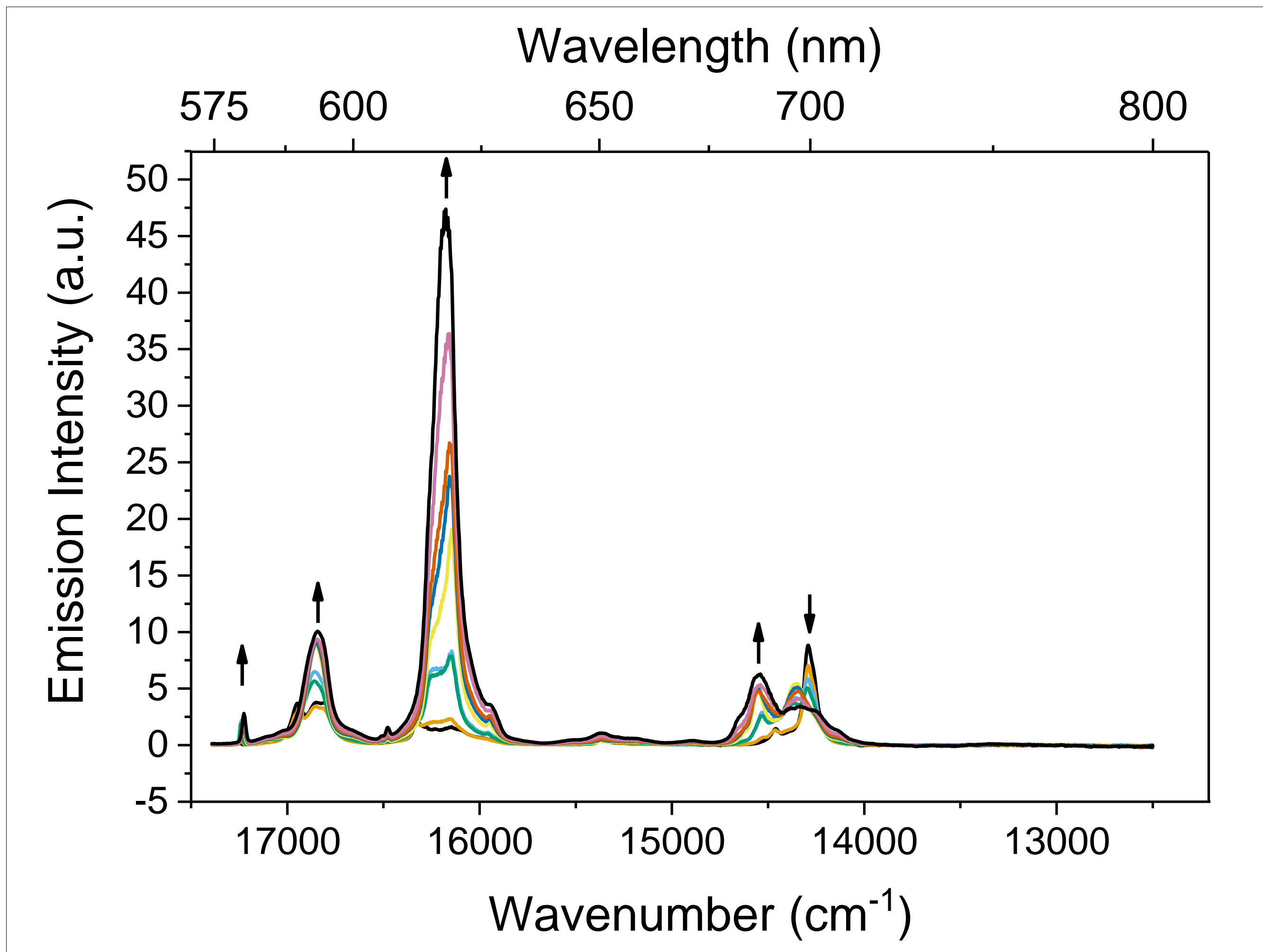
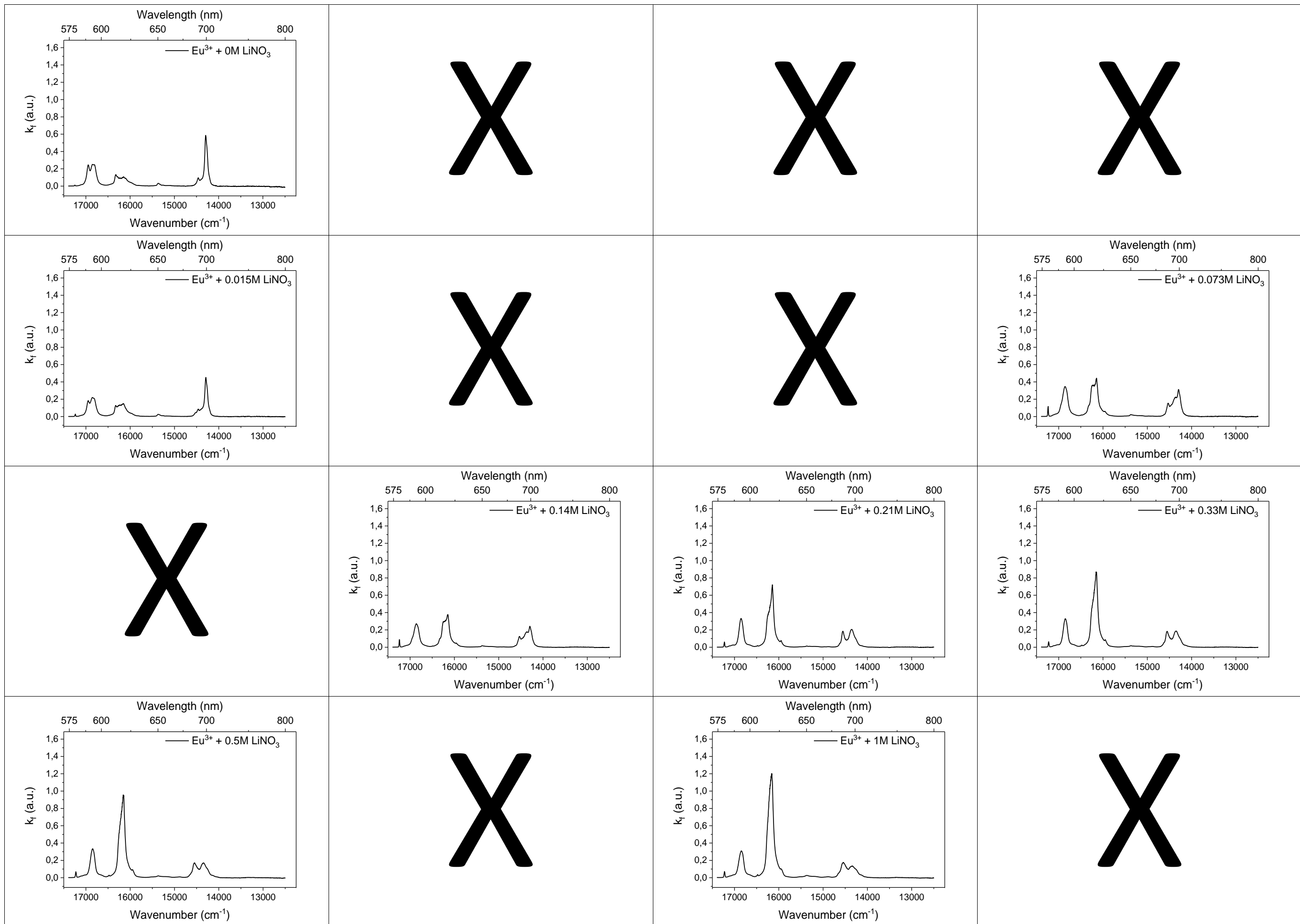


Figure S4: Emission spectra of 0.1M $\text{Eu}(\text{CF}_3\text{SO}_3)_3$ in MeOH with concentrations of LiNO_3 from 0 to 2M at 20°C , excited at 394nm . Emission and excitation slits were kept at 0.4 and 8 nm respectively. Intensity was corrected for wavelength dependent detector sensibility and lamp intensity with a reference detector and factory supplied correction files. Arrows indicate changes in emission intensity as a function of increasing LiNO_3 .



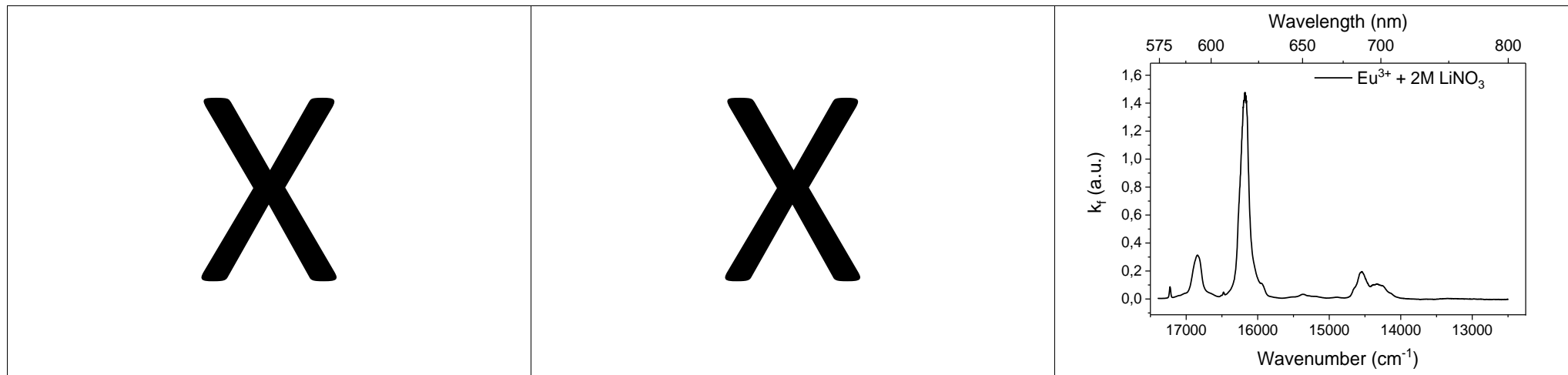


Figure S5: Rate of emission (see main text for details) of 0.1M $\text{Eu}(\text{CF}_3\text{SO}_3)_3$ in MeOH with concentrations of LiNO_3 from 0 to 2M at 20 °C, excited at 394nm. Emission and excitation slits were kept at 0.4 and 8 nm respectively. Emission spectra was corrected for changes in absorption at the excitation wavelength and non-radiative processes (see main text) as well as wavelength dependent detector sensibility and lamp intensity with a reference detector and factory supplied correction files

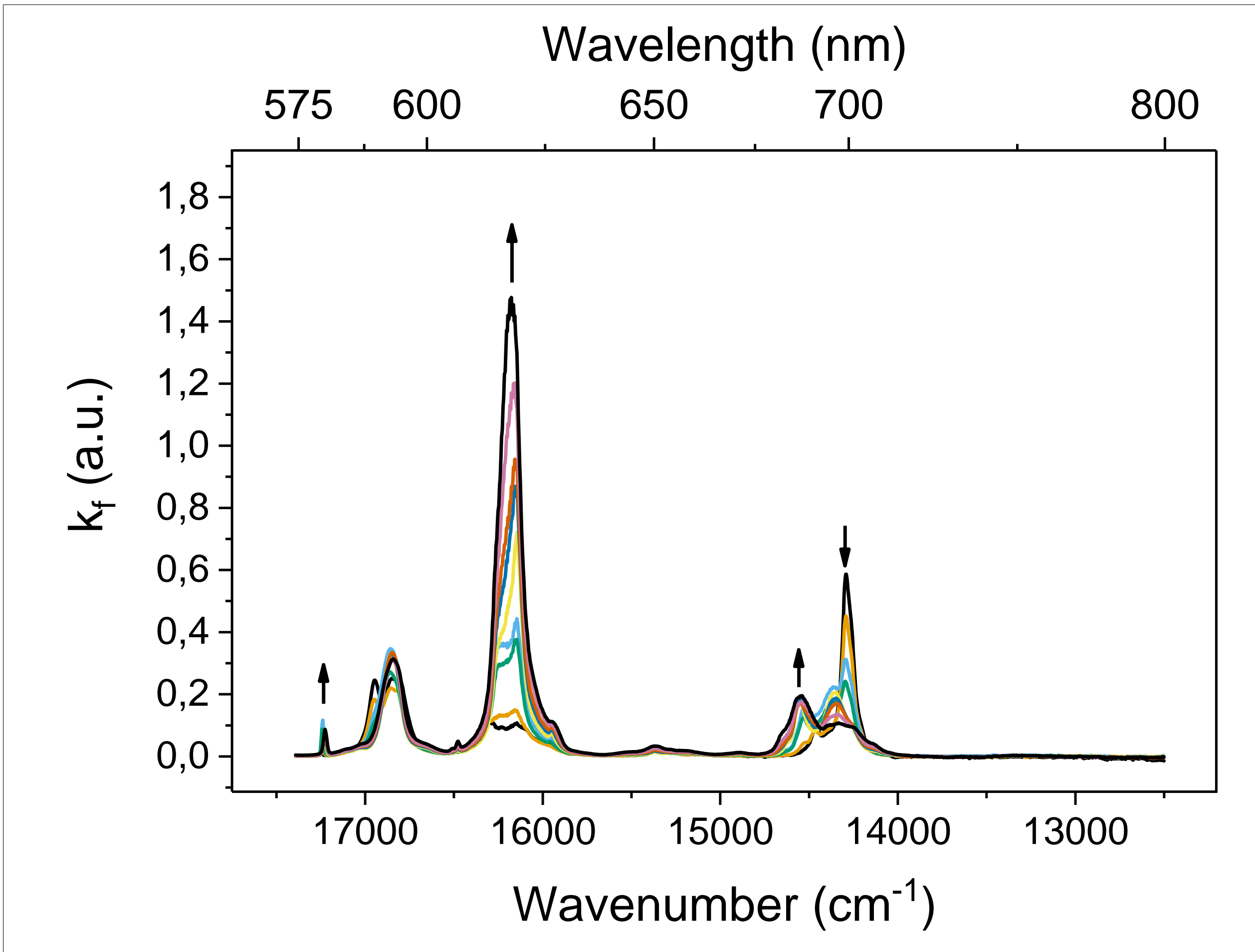


Figure S6: Relative rate of emission (see main text for details) of 0.1M $\text{Eu}(\text{CF}_3\text{SO}_3)_3$ in MeOH with concentrations of LiNO_3 from 0 to 2M at 20 °C, excited at 394nm. Emission and excitation slits were kept at 0.4 and 8 nm respectively. Emission spectra was corrected for changes in absorption at the excitation wavelength and non-radiative processes (see main text) as well as wavelength dependent detector sensibility and lamp intensity with a reference detector and factory supplied correction files. Arrows indicate changes in the rate constant as a function of increasing LiNO_3 .

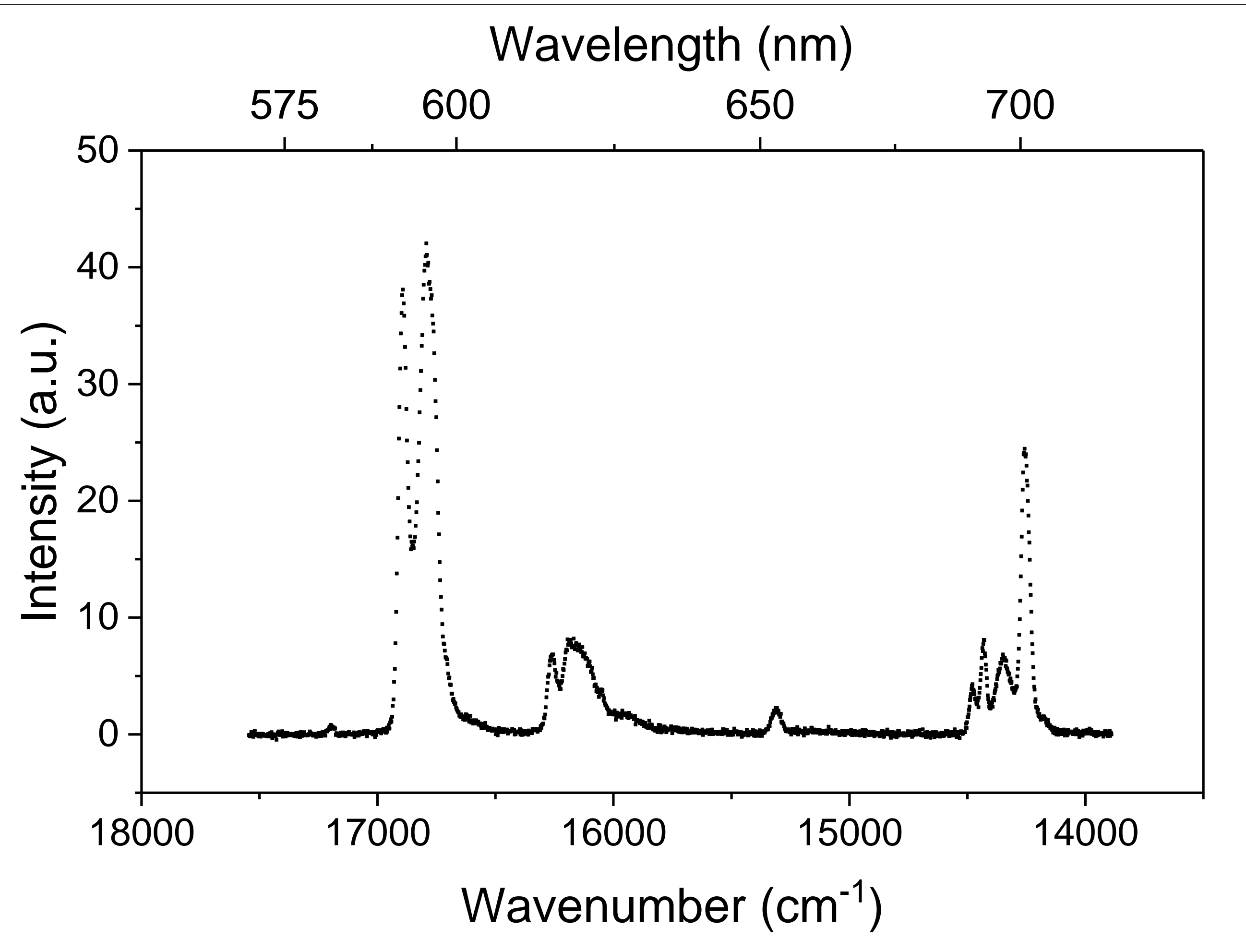
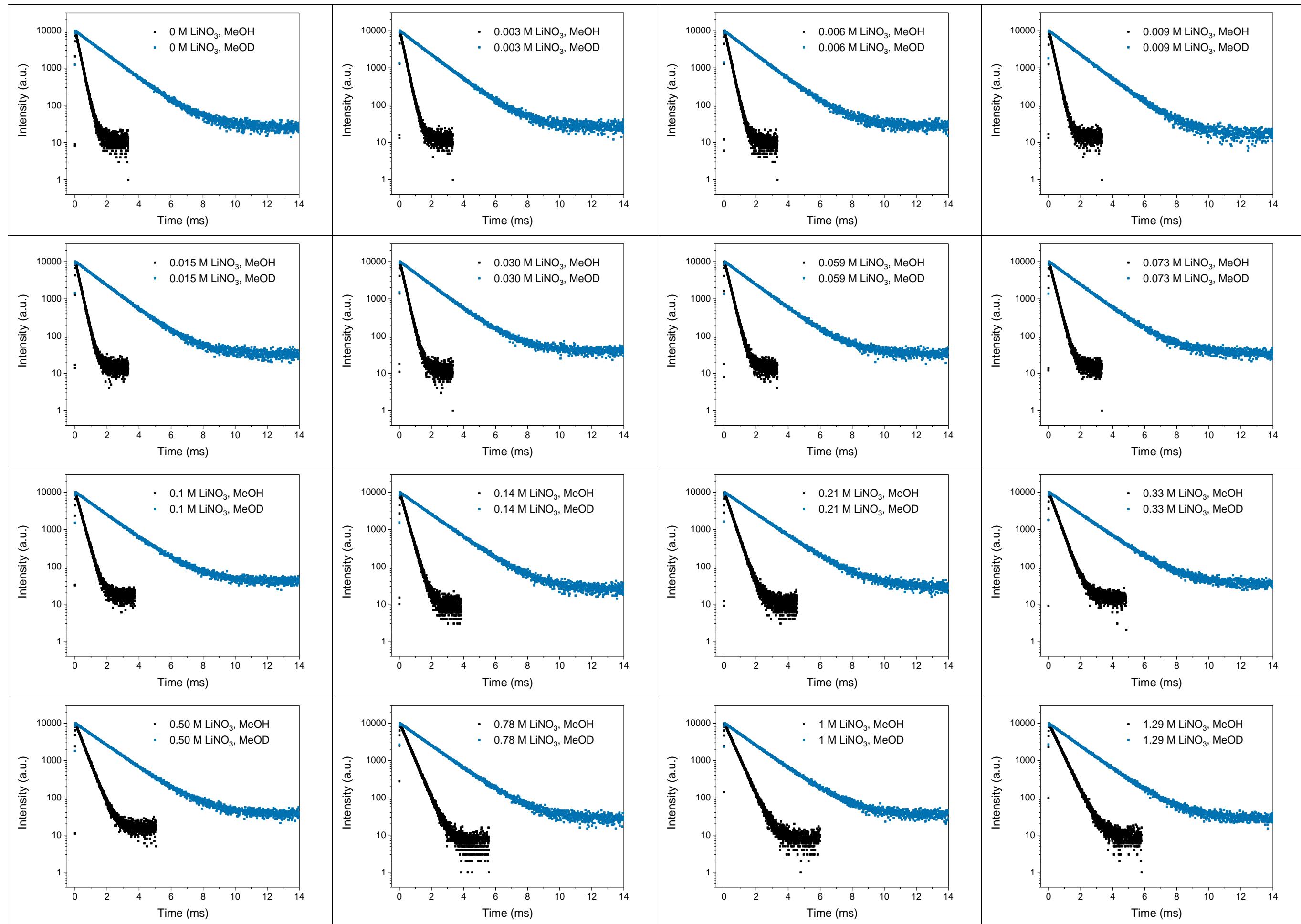


Figure S7: Time-gated emission spectra of 0.1M Eu(CF₃SO₃)₃ in MeOH-d₄ flash frozen in liquid nitrogen at 77K. Excitation was done at 394 nm and slits were kept at 8 and 1 nm for excitation and emission slits respectively. The time-gate was set at 200-5000ms to avoid scattered light. Intensity was corrected for wavelength dependent detector sensibility and lamp intensity with a reference detector and factory supplied correction files.

Lifetime traces

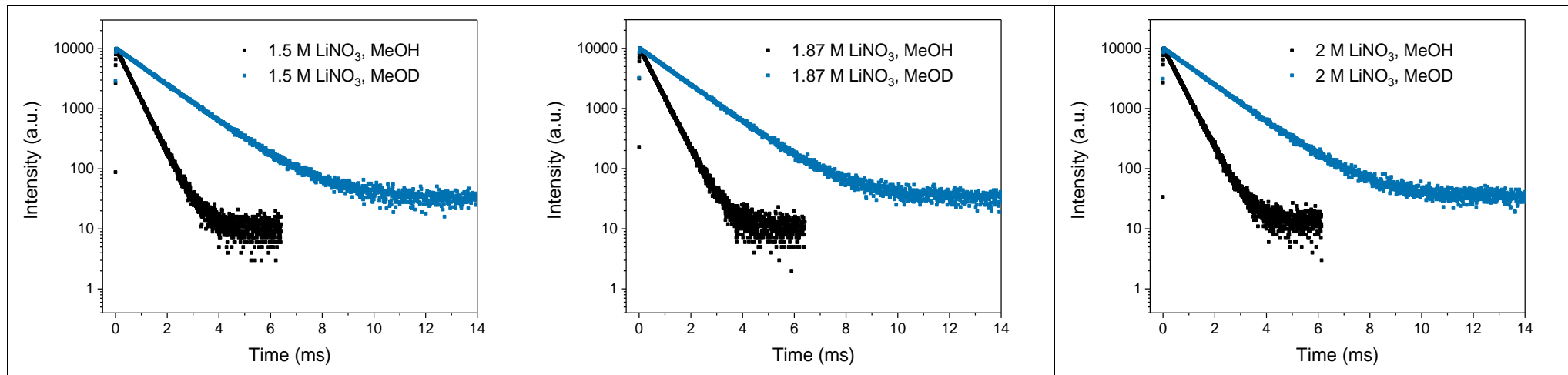
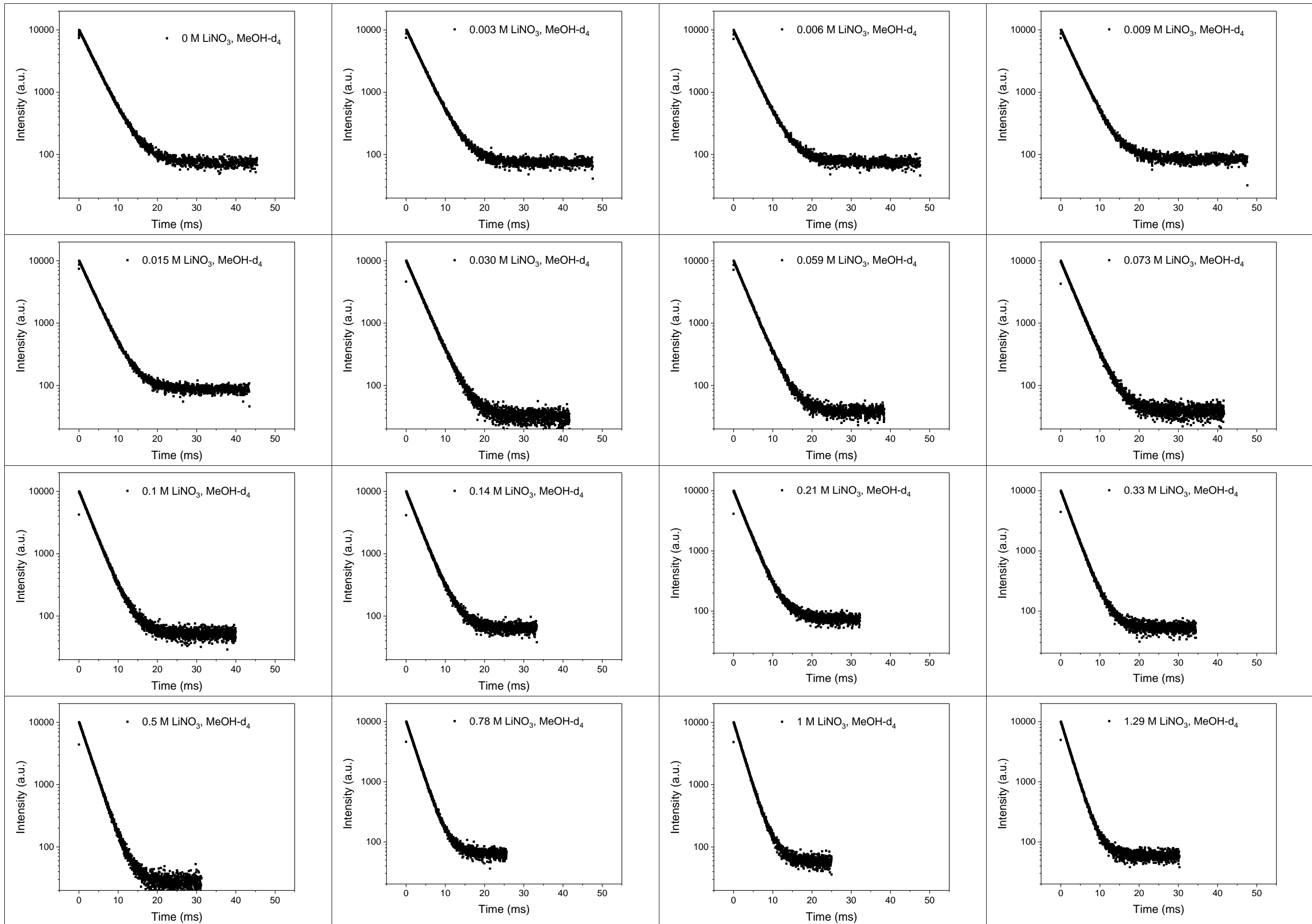


Figure S8: Decay traces of 0.1M Eu(CF₃SO₃)₃ in MeOH/MeOD with concentrations of LiNO₃ from 0 to 2M at 20 °C. Emission and excitation slits were both kept at 5 nm. Excitation was done at 394 nm and emission was detected at 698 nm.



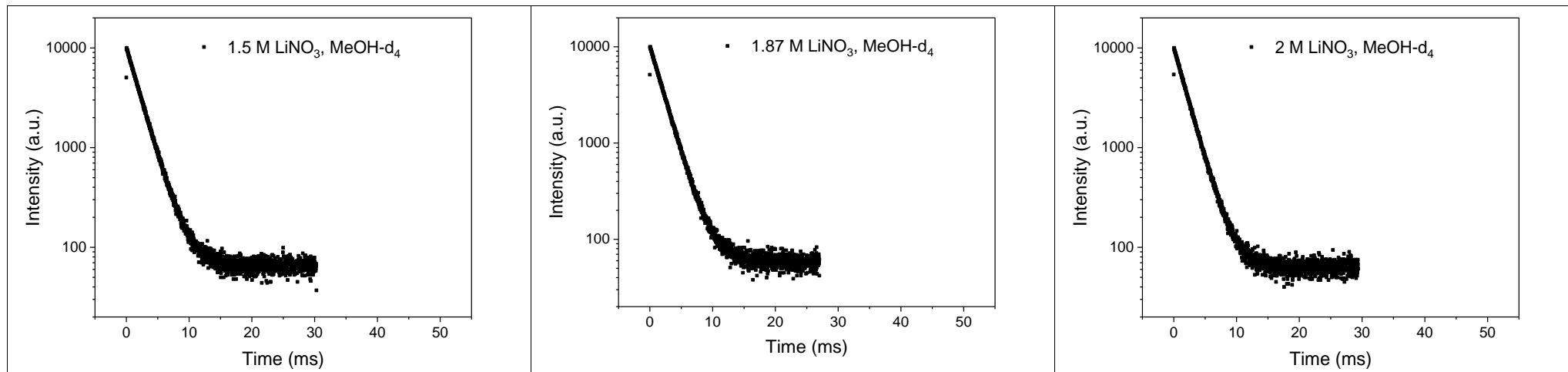
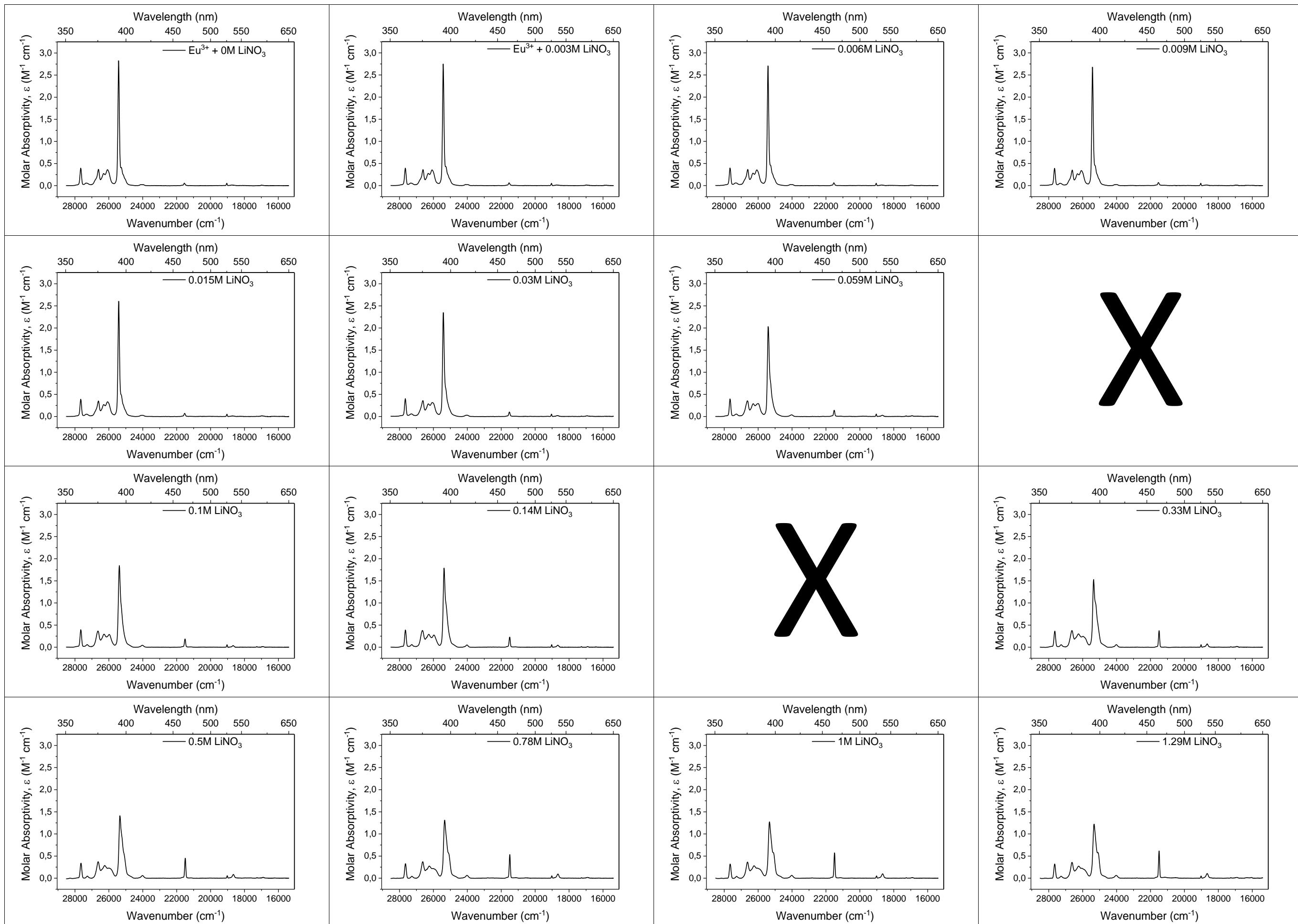
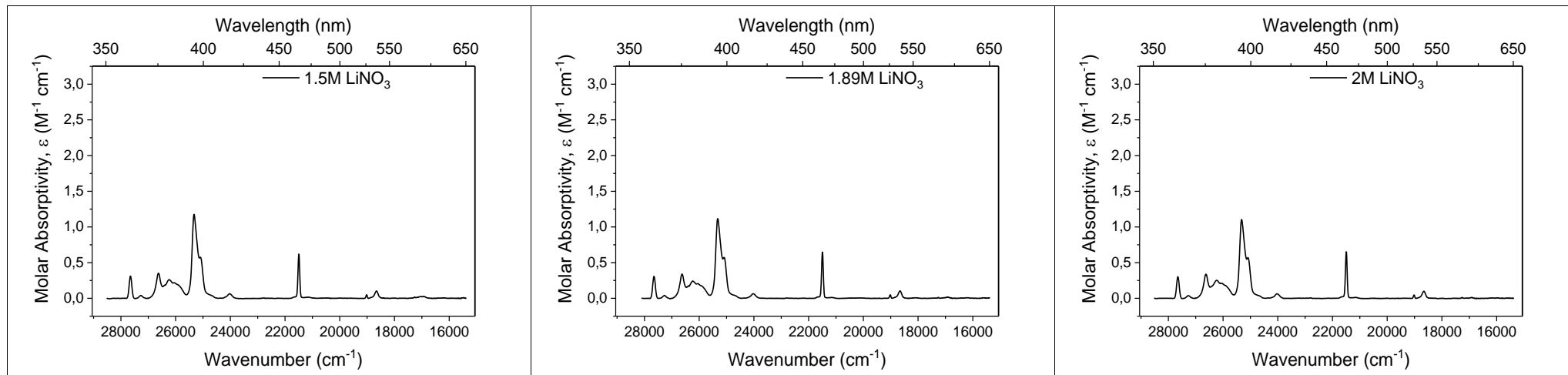


Figure S9: Lifetime traces of 0.1M $\text{Eu}(\text{CF}_3\text{SO}_3)_3$ in MeOH-d_4 with LiNO_3 from 0 to 2M at 20 °C. Emission and excitation slits were both kept at 5 nm. Excitation was done at 394 nm and emission was detected at 620 nm.

Table S1: Fits of decay traces of $\text{Eu}(\text{CF}_3\text{SO}_3)_3$ in MeOH , MeOD and MeOH-d_4 with LiNO_3 from 0 to 2M. All traces were fitted to a mono-exponential decay and showed no second component.

Sample	A (a.u.), MeOH	T (ms), MeOH	A (a.u.), MeOD	T (ms), MeOD	A (a.u.), MeOH-d_4	T (ms), MeOH-d_4
$\text{Eu}^{3+} + 0 \text{M LiNO}_3$	11415	0.2138	10088	1.356	10036	3.336
$\text{Eu}^{3+} + 0.003 \text{M LiNO}_3$	11558	0.2184	10109	1.331	10154	3.234
$\text{Eu}^{3+} + 0.006 \text{M LiNO}_3$	9620	0.2637	9678	1.378	9729	3.233
$\text{Eu}^{3+} + 0.009 \text{M LiNO}_3$	9569	0.2653	9843	1.377	10041	3.199
$\text{Eu}^{3+} + 0.015 \text{M LiNO}_3$	9445	0.2670	9933	1.385	9950	3.185
$\text{Eu}^{3+} + 0.030 \text{M LiNO}_3$	9493	0.2750	9950	1.395	9870	3.048
$\text{Eu}^{3+} + 0.059 \text{M LiNO}_3$	9591	0.2911	9980	1.419	9945	2.923
$\text{Eu}^{3+} + 0.073 \text{M LiNO}_3$	9485	0.3010	9889	1.425	9752	2.928
$\text{Eu}^{3+} + 0.1 \text{M LiNO}_3$	9573	0.3221	9983	1.457	9958	2.833
$\text{Eu}^{3+} + 0.14 \text{M LiNO}_3$	9668	0.3306	9908	1.493	9866	2.785
$\text{Eu}^{3+} + 0.21 \text{M LiNO}_3$	9724	0.3833	9925	1.528	9839	2.730
$\text{Eu}^{3+} + 0.33 \text{M LiNO}_3$	9909	0.4057	9963	1.514	9882	2.523
$\text{Eu}^{3+} + 0.5 \text{M LiNO}_3$	9921	0.4268	9886	1.492	10032	2.380
$\text{Eu}^{3+} + 0.78 \text{M LiNO}_3$	9977	0.4637	9951	1.471	9953	2.246
$\text{Eu}^{3+} + 1.00 \text{M LiNO}_3$	9945	0.4854	9966	1.480	9956	2.163
$\text{Eu}^{3+} + 1.29 \text{M LiNO}_3$	9882	0.5123	9783	1.460	9952	2.097
$\text{Eu}^{3+} + 1.50 \text{M LiNO}_3$	9955	0.5281	10007	1.457	9843	2.059
$\text{Eu}^{3+} + 1.87 \text{M LiNO}_3$	9965	0.5455	9934	1.447	9887	2.020
$\text{Eu}^{3+} + 2.00 \text{M LiNO}_3$	9892	0.5536	9896	1.448	9836	1.982

Absorption, MeOH-d₄



FigureS10: Absorption of 0.1 M Eu(CF₃SO₃)₃ in MeOH-d₄ with concentrations of LiNO₃ from 0 to 2M at room temperature. Slits were kept at 1 nm.

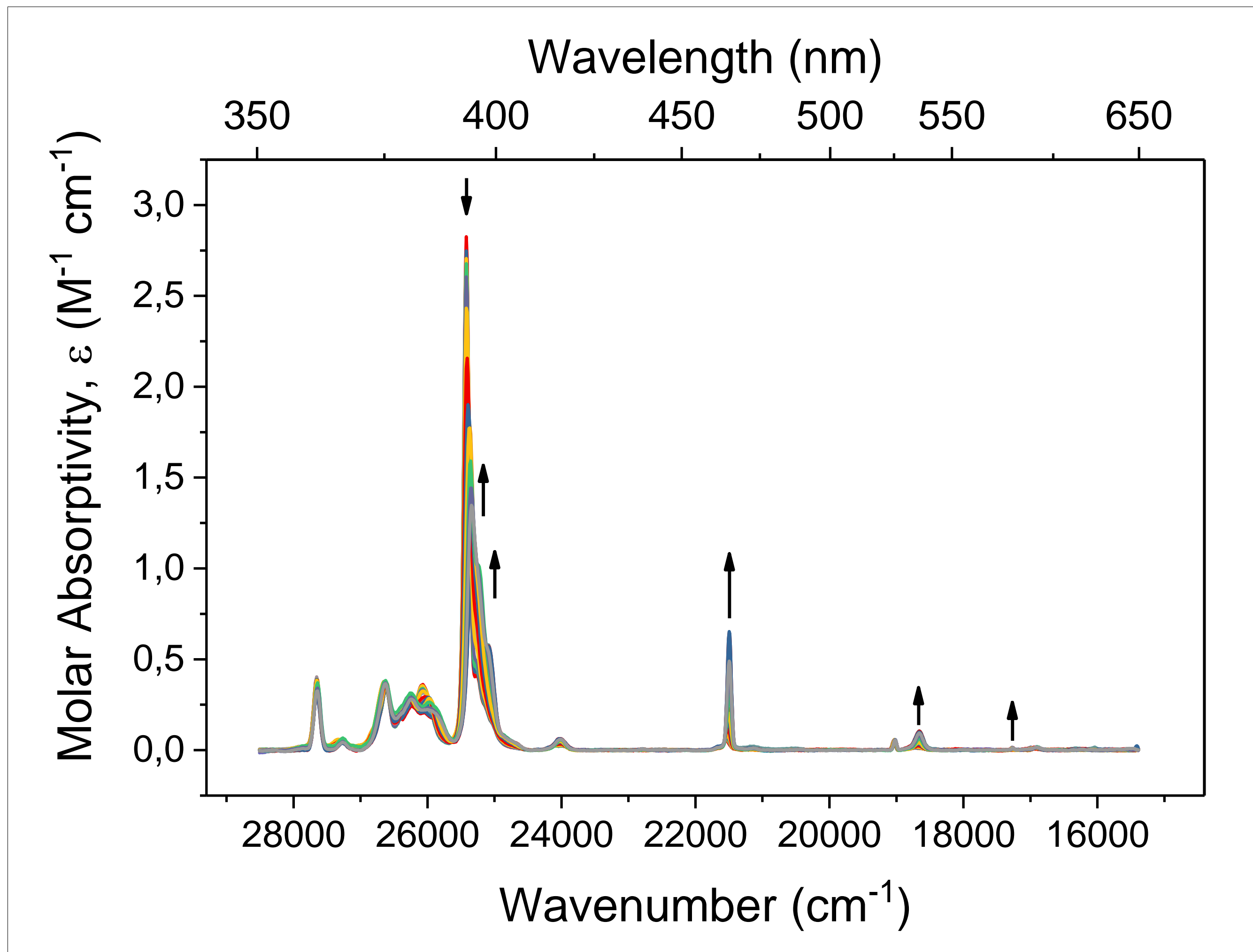
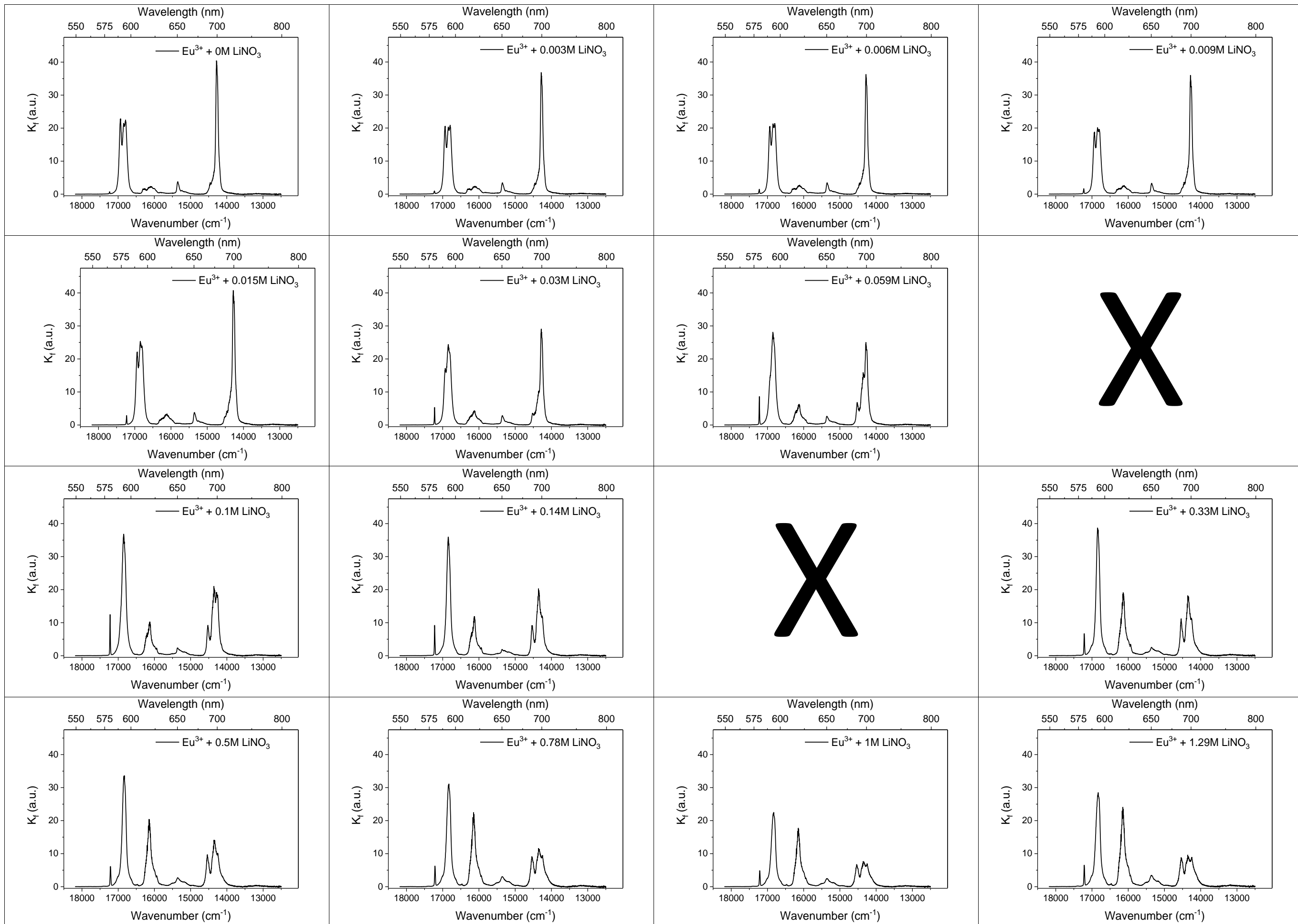
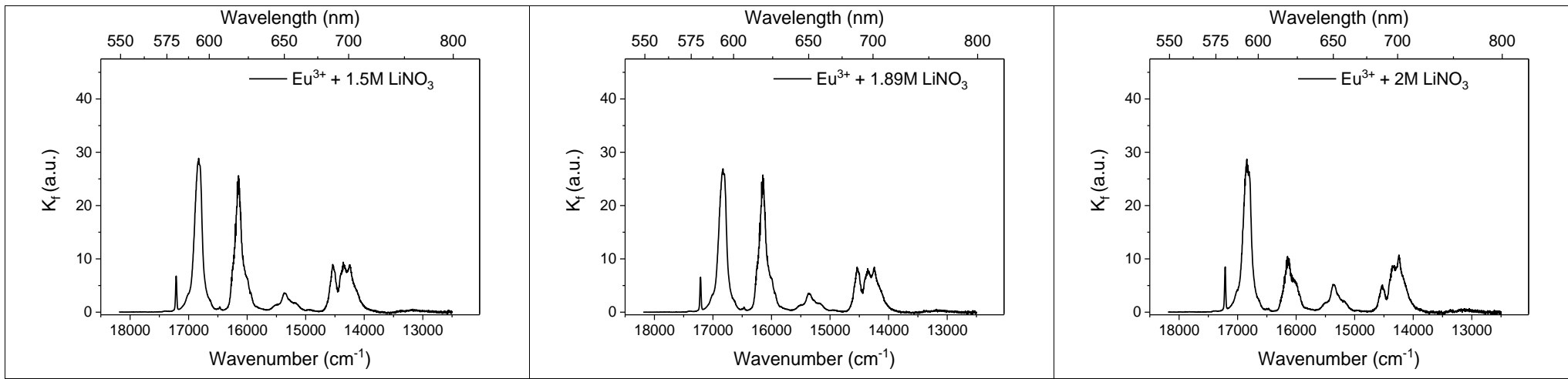


Figure S11: Absorption of 0.1 M $\text{Eu}(\text{CF}_3\text{SO}_3)_3$ in MeOH-d_4 with concentrations of LiNO_3 from 0 to 2M at RT. Slits were kept at 1 nm. Arrows indicate changes in absorption as a function of increasing LiNO_3 .

Emission, MeOH-d₄



FigureS12: Relative rate of emission (see main text for details) of 0.1 M $\text{Eu}(\text{CF}_3\text{SO}_3)_3$ in MeOH-d_4 with concentrations of LiNO_3 from 0 to 2M at 20 °C. Slits were kept at 8 and 0.4 nm for excitation and emission slits respectively. Emission spectra was corrected for changes in absorption at the excitation wavelength and non-radiative processes (see main text) as well as wavelength dependent detector sensibility and lamp intensity with a reference detector and factory supplied correction files.

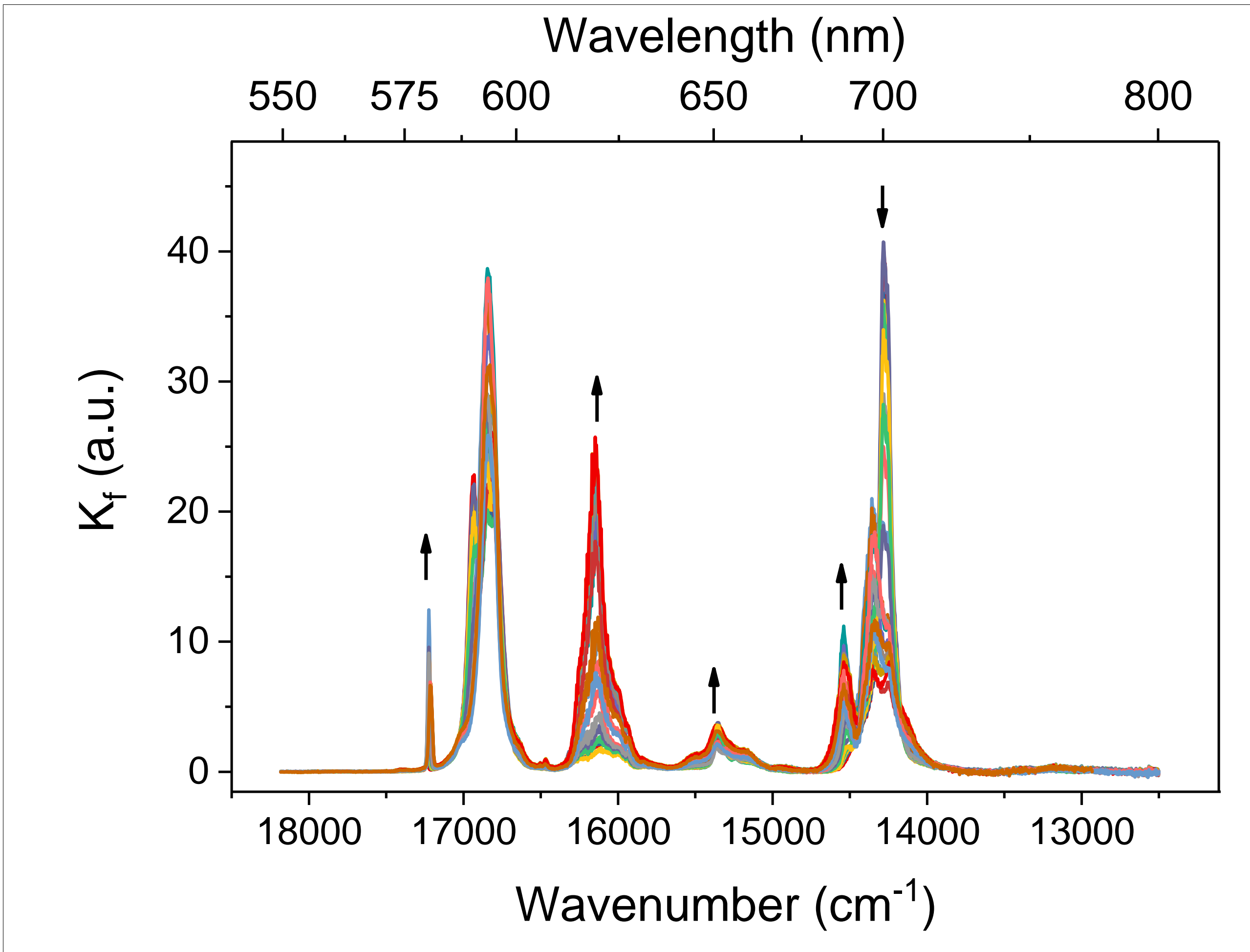
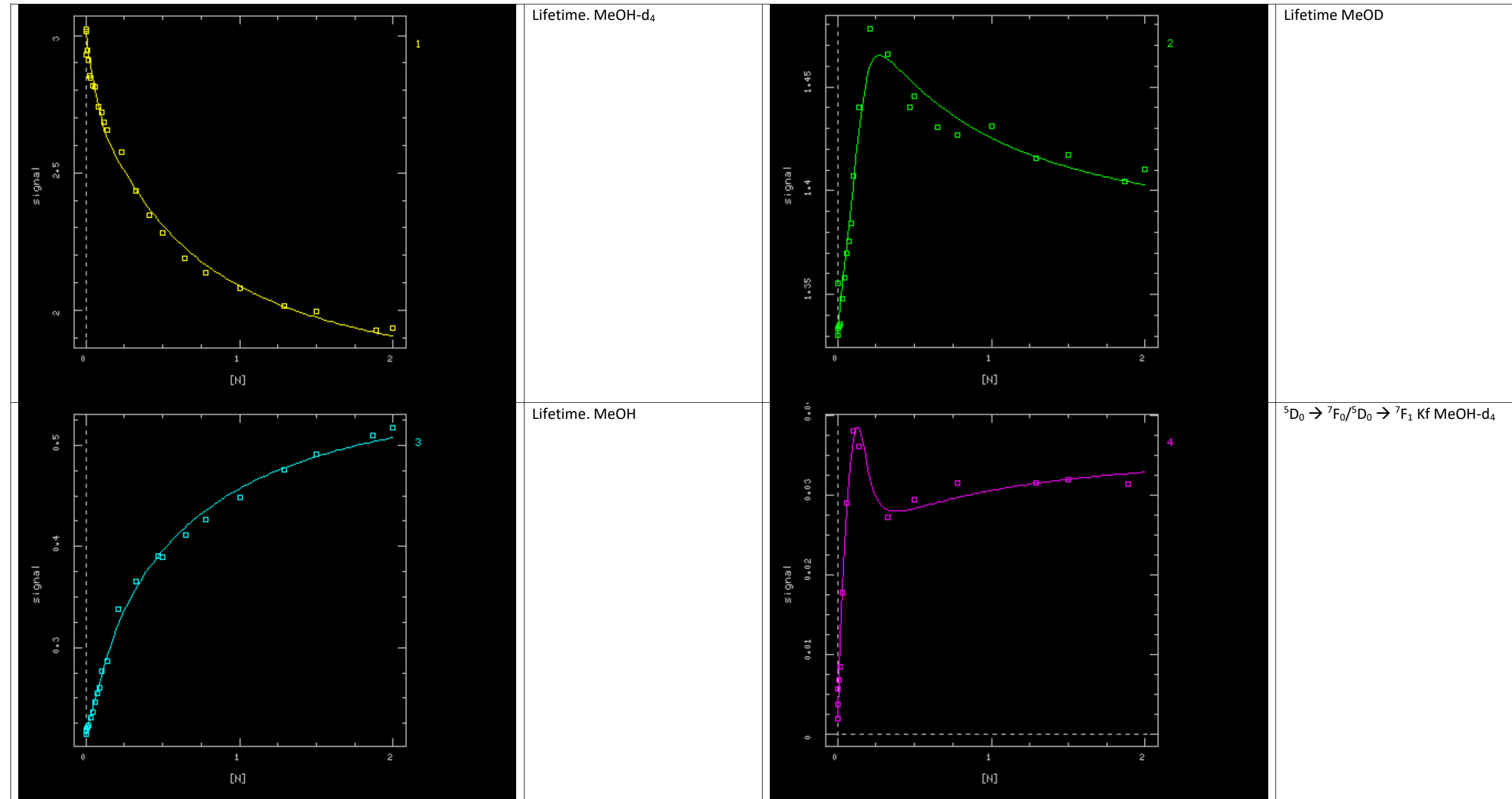
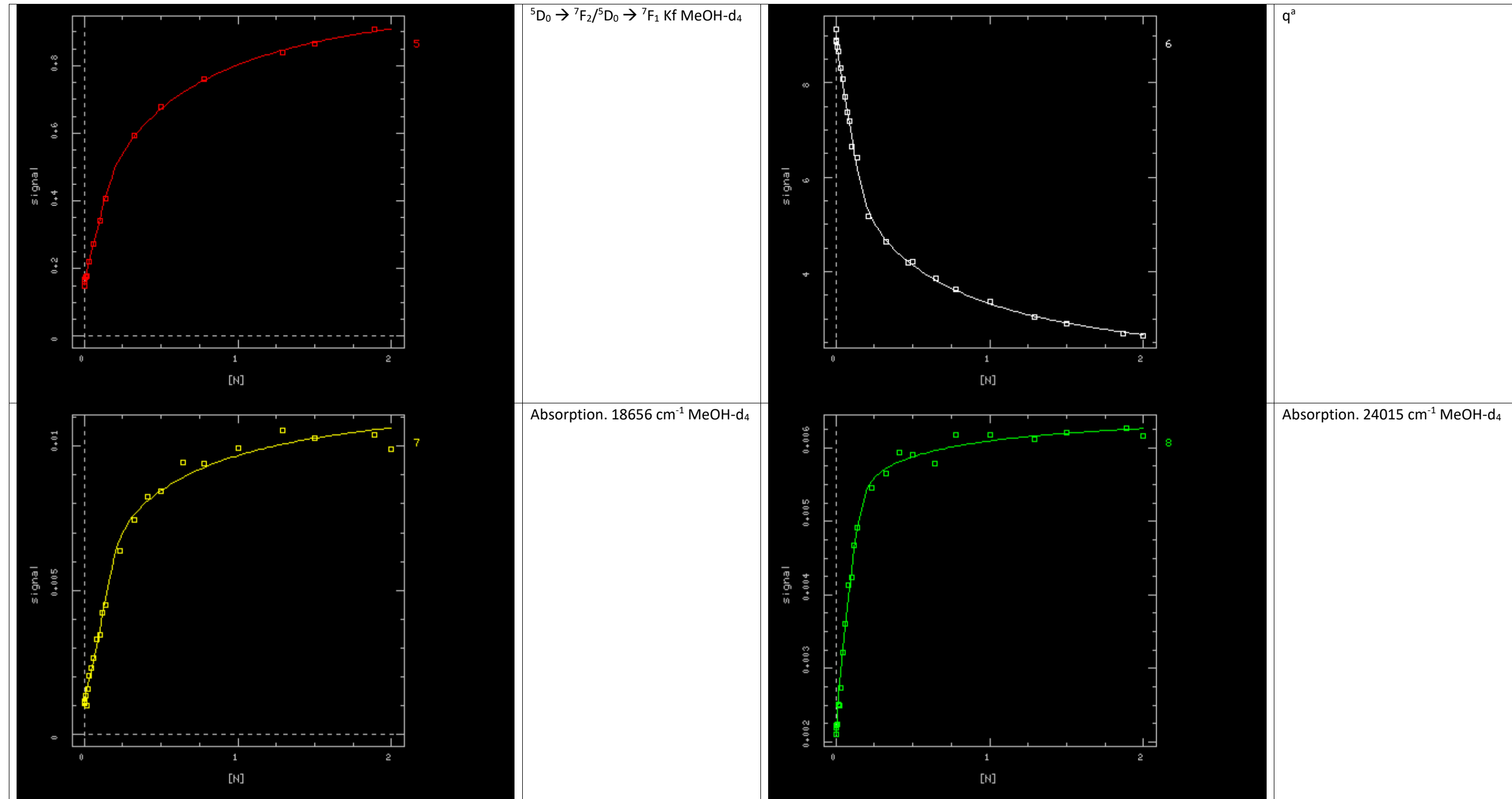


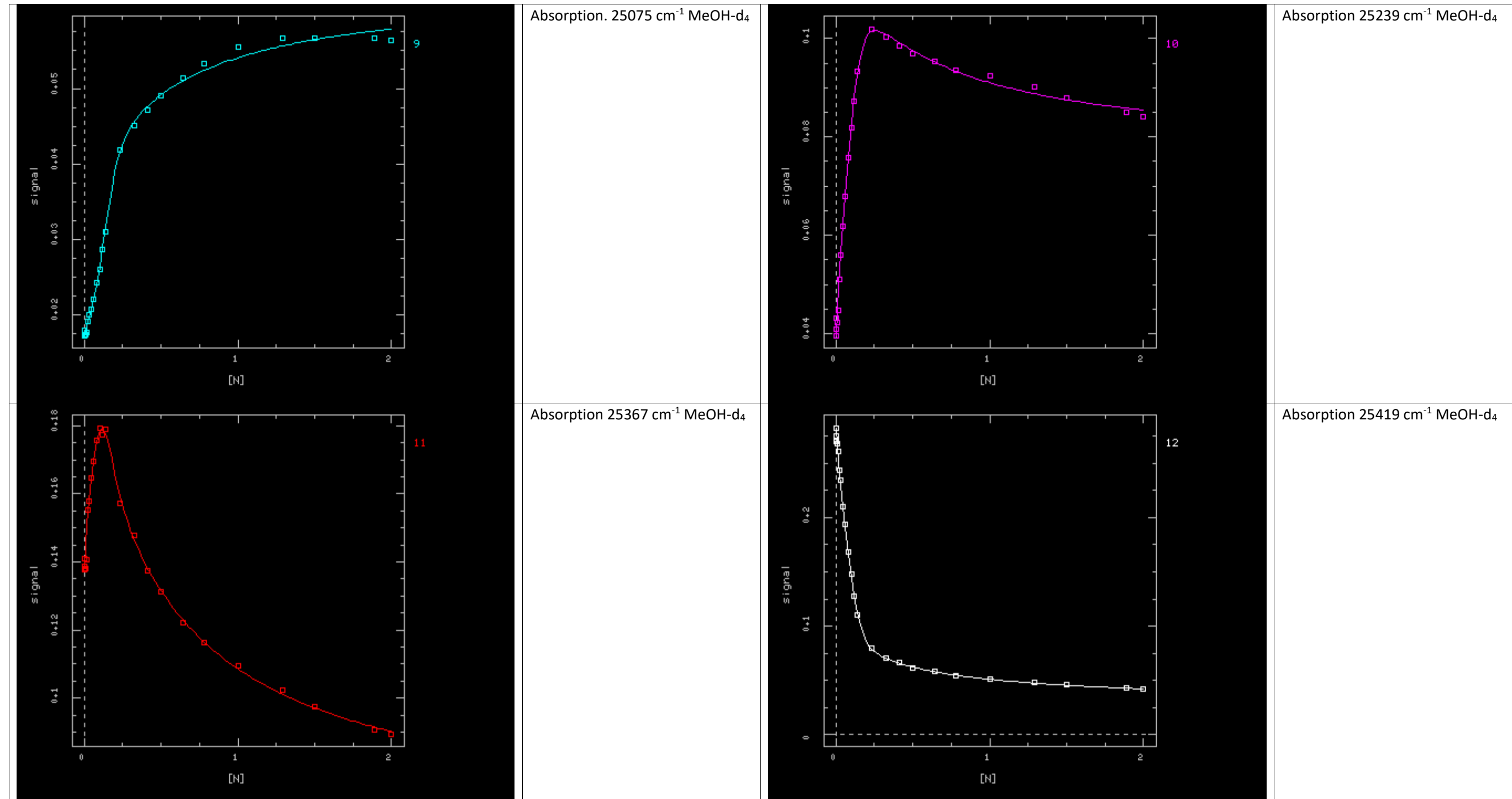
Figure S13: Rate of emission of 0.1 M $\text{Eu}(\text{CF}_3\text{SO}_3)_3$ in MeOH-d_4 with concentrations of LiNO_3 from 0 to 2M at 20 °C. Slits were kept at 8 and 0.4 nm for excitation and emission slits respectively. Emission spectra was corrected for changes in absorption at the excitation wavelength and non-radiative processes (see main text) as well as wavelength dependent detector sensibility and lamp intensity with a reference detector and factory supplied correction files. Arrows indicate changes in the relative rate constant as a function of increasing LiNO_3 .

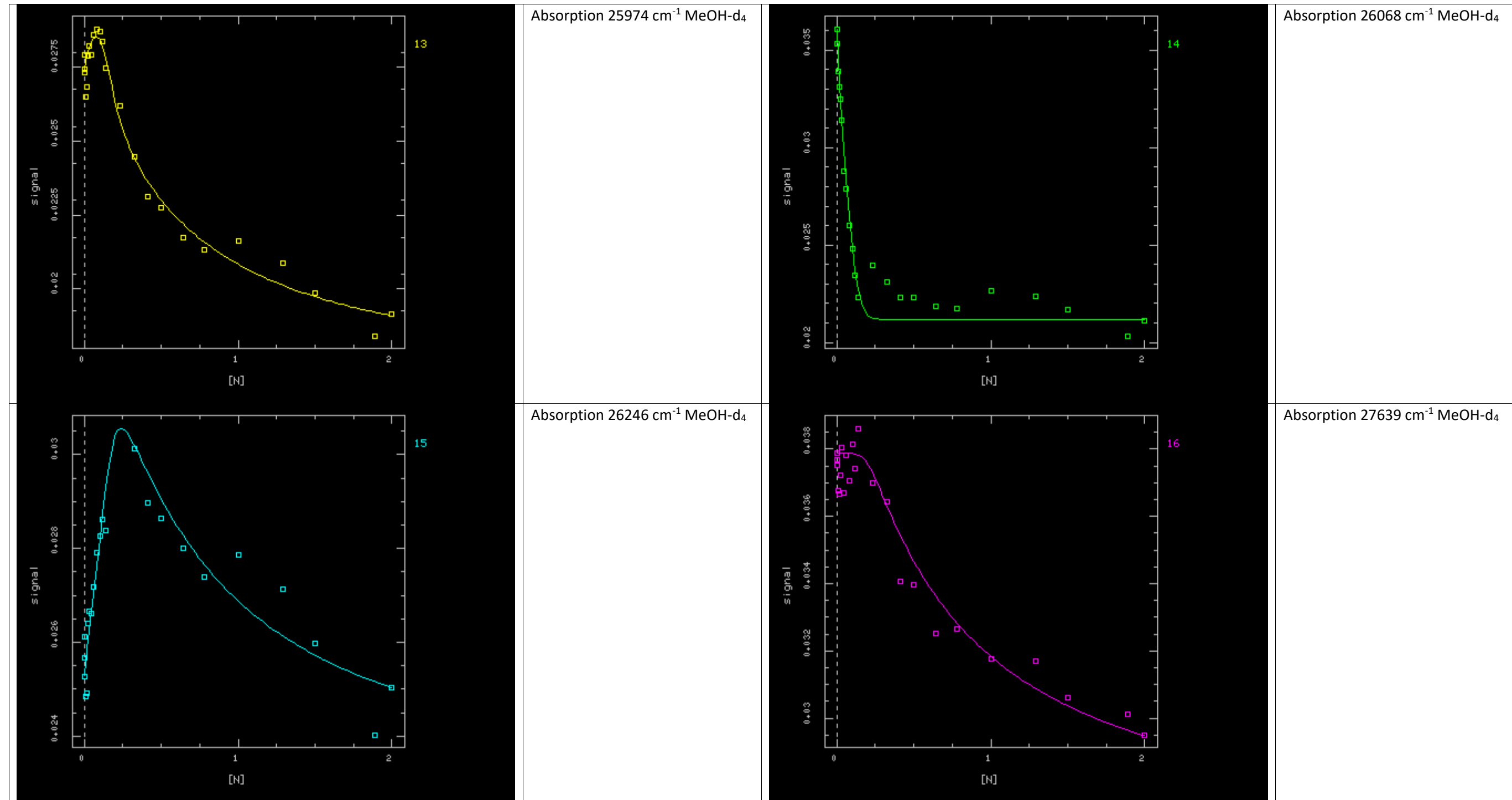
Speciation Modelling

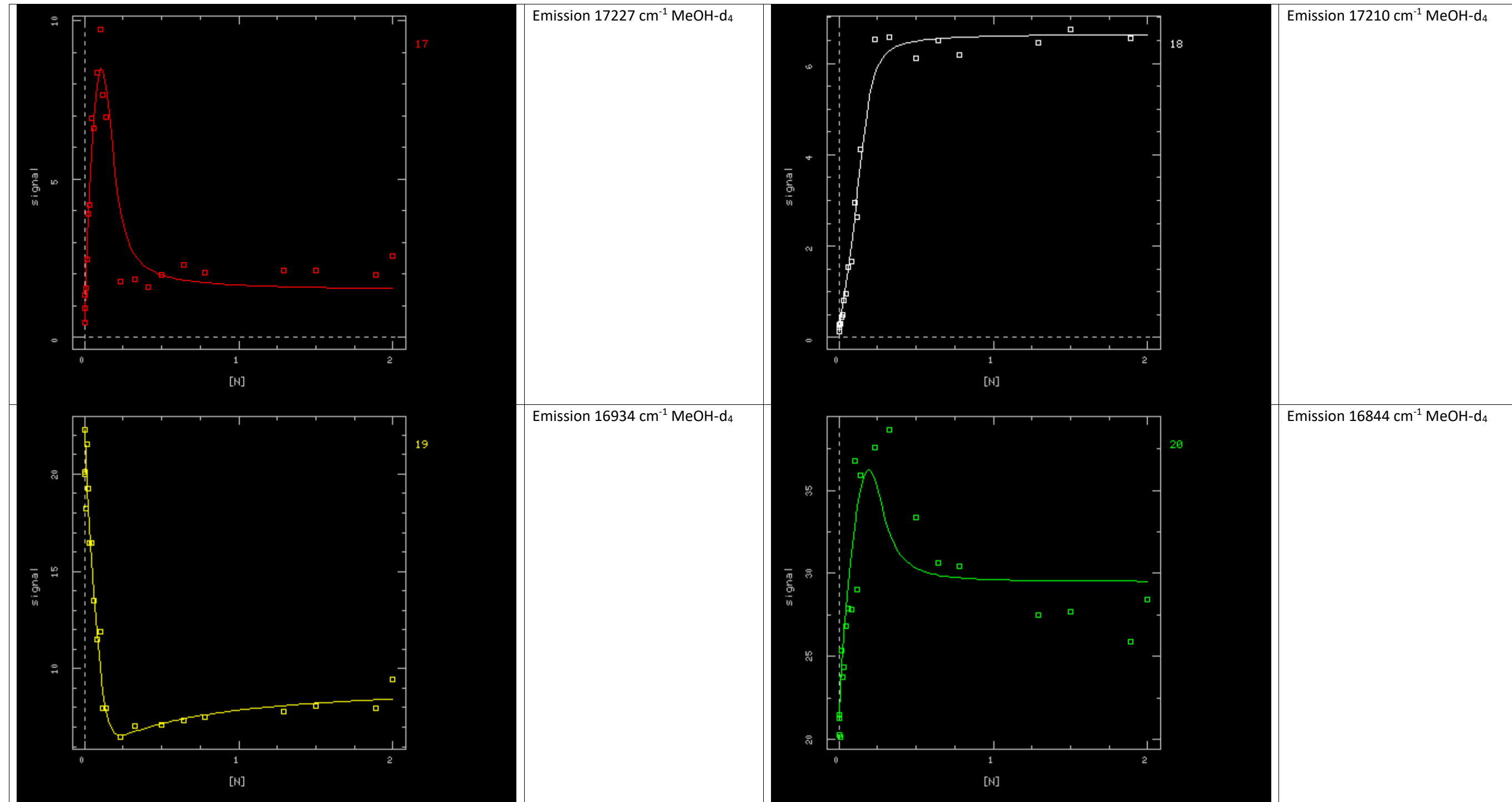
Dynafit Traces and Fits

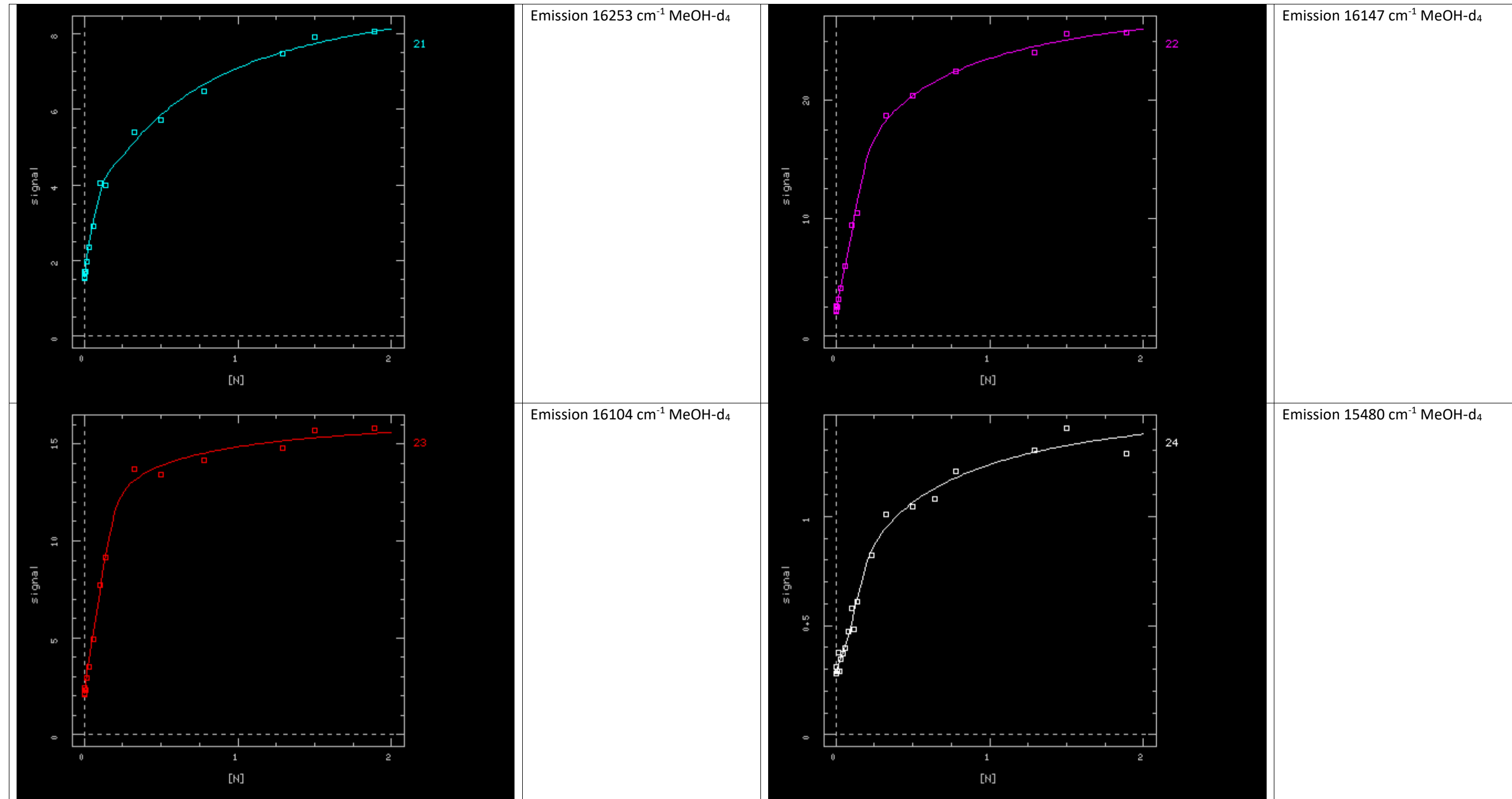


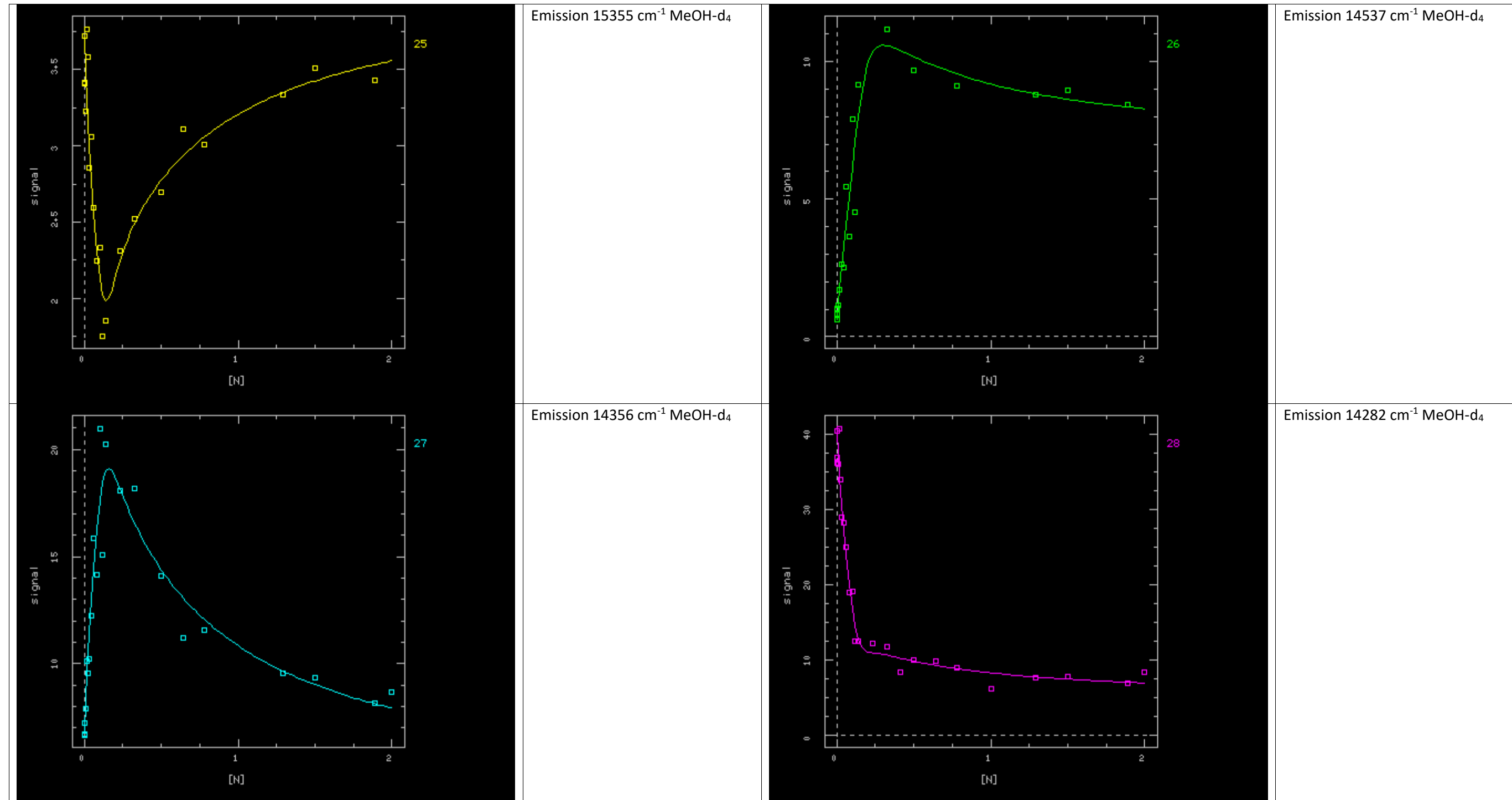












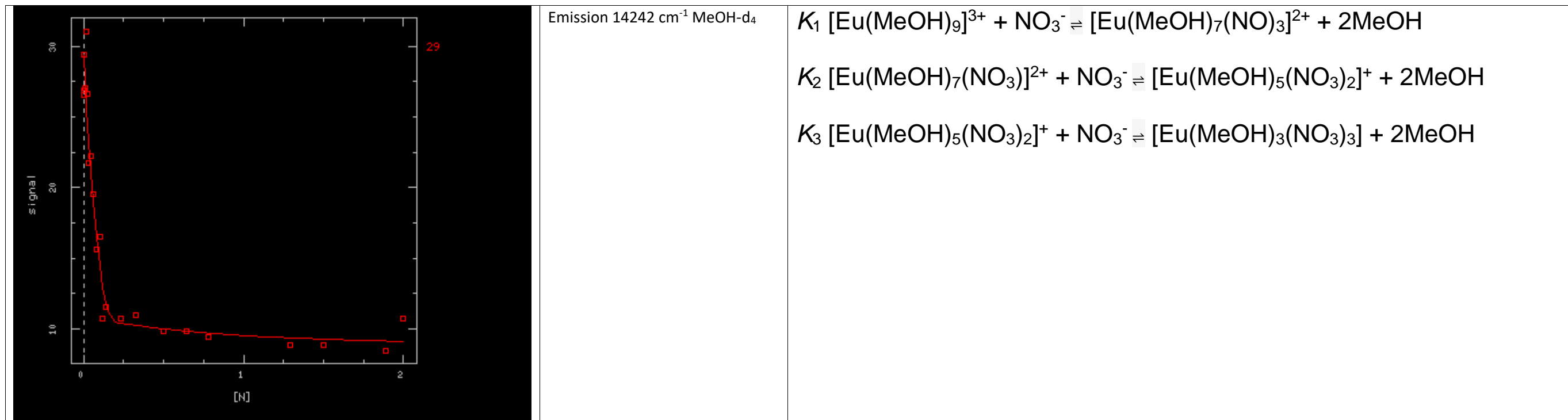


Figure S14: Data used for fitting binding constants in Dynafit. All sets are as a function of concentrations of LiNO₃. The three equilibria model was used for the fit.^a q from Horrocks Equation¹⁻³. Binding constants were modelled from absorption data. Emission data was modelled using the binding constants found from absorption data (see main text for details). Including a fourth equilibrium did not allow for convergence

Confidence interval profiles from Dynafit

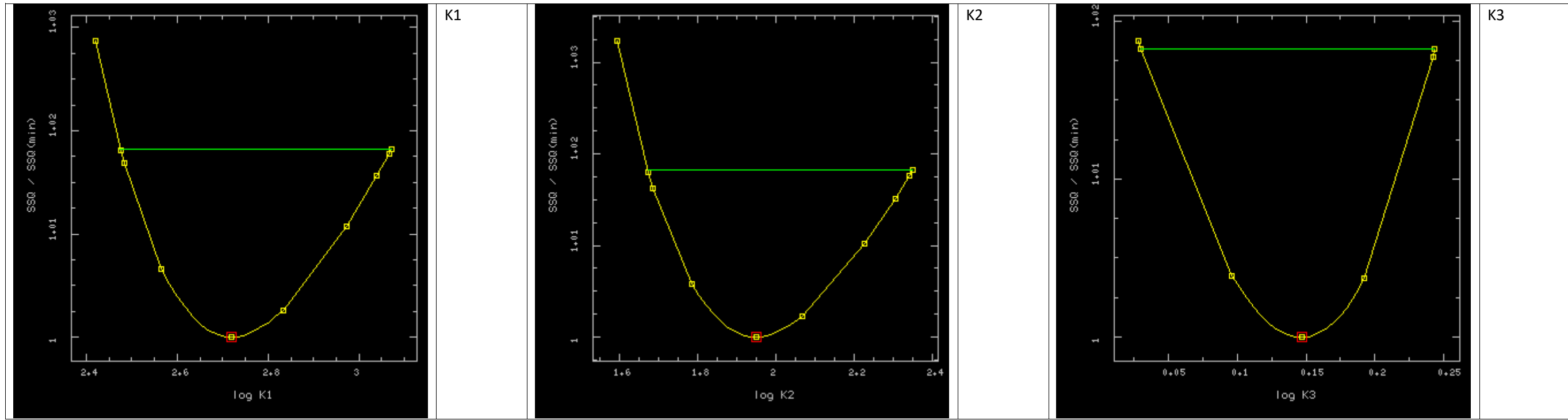


Figure S15: Confidence interval profiles (95%) of K1, K2 and K3 from Dynafit. See Figure S14 and main text for details

Best Fit Parameters

Table S2: Parameter set for fitting procedure used in Dynafit, see Figure S14 and S15

Parameter name	Initial	Final	Standard Error	CV (%)	Low ^a	High ^a
K1	524.339	520	160	30.5	300	1200
K2	88.7807	89	28	31.8	47	220
K3	1.40265	1.4	0.16	11.2	1.07	1.75
Lifetime, MeOH-d ₄ (1)	2.713	2.61	0.7	26.9		
Lifetime, MeOH-d ₄ (2)	2.43	2.56	0.6	23.3		
Lifetime, MeOH-d ₄ (3)	1.99	1.63	0.72	44.3		
Lifetime, MeOD (1)	1.407	1.4	0.71	50.5		
Lifetime, MeOD (2)	1.465	1.49	0.62	41.8		
Lifetime, MeOD (3)	1.41	1.37	0.74	53.7		
Lifetime, MeOH (1)	0.275	0.27	0.71	261.9		
Lifetime, MeOD (2)	0.368	0.33	0.62	188.9		
Lifetime, MeOD (3)	0.5	0.58	0.74	126.8		
F0/F1 Emission (1)	0.04	0.058	0.97	1673.6		
F0/F1 Emission (2)	0.025	0.024	0.87	3630.8		
F0/F1 Emission (3)	0.03	0.036	0.96	2663.3		
F2/F1 Emission (1)	0.3	0.36	0.97	269.6		
F2/F1 Emission (2)	0.6	0.53	0.87	164.4		
F2/F1 Emission (3)	1	1.07	0.96	89.6		
q (1)	6.64	6.64	0.71	10.7		
q (2)	4.974	4.97	0.62	12.5		
q (3)	1.704	1.7	0.74	43.3		
5D0 Absorption (1)	0.055	0.095	0.89	941.3		
5D0 Absorption (2)	0.04	0.043	0.31	727.5		
5D0 Absorption (3)	0.6	0.61	0.39	63.6		
5D2 Absorption (1)	1.5	1.6	1.1	66.9		
5D2 Absorption (2)	3.1	2.77	0.85	30.5		
5D2 Absorption (3)	5	5.99	0.82	13.6		
Absorption, 18656 cm ⁻¹ (1)	0.0034	0.0033	0.7	21249.1		
Absorption, 18656 cm ⁻¹ (2)	0.0073	0.0073	0.6	8179.7		
Absorption, 18656 cm ⁻¹ (3)	0.0119	0.012	0.72	6013.0		
Absorption, 24015 cm ⁻¹ (1)	0.0048	0.0048	0.7	14608.7		
Absorption, 24015 cm ⁻¹ (2)	0.0057	0.0057	0.6	10475.8		
Absorption, 24015 cm ⁻¹ (3)	0.0065	0.0065	0.72	11100.9		
Absorption, 25075 cm ⁻¹ (1)	0.02546	0.024	0.7	2921.7		
Absorption, 25075 cm ⁻¹ (2)	0.0418	0.045	0.6	1326.9		
Absorption, 25075 cm ⁻¹ (3)	0.06	0.063	0.72	1145.3		
Absorption, 25239 cm ⁻¹ (1)	0.0934	0.094	0.7	746.0		
Absorption, 25239 cm ⁻¹ (2)	0.1064	0.11	0.6	542.8		
Absorption, 25239 cm ⁻¹ (3)	0.0782	0.077	0.72	937.1		
Absorption, 25267 cm ⁻¹ (1)	0.2035	0.21	0.7	333.9		
Absorption, 25267 cm ⁻¹ (2)	0.1554	0.15	0.6	398.1		
Absorption, 25267 cm ⁻¹ (3)	0.066	0.063	0.72	1145.3		
Absorption, 25419 cm ⁻¹ (1)	0.1112	0.11	0.7	637.5		
Absorption, 25419 cm ⁻¹ (2)	0.0731	0.073	0.6	818.0		
Absorption, 25419 cm ⁻¹ (3)	0.0309	0.029	0.72	2488.1		
Absorption, 25974 cm ⁻¹ (1)	0.03	0.03	0.7	2337.4		
Absorption, 25974 cm ⁻¹ (2)	0.02527	0.025	0.6	2388.5		
Absorption, 25974 cm ⁻¹ (3)	0.0168	0.017	0.72	4244.5		
r(C3)#17	0.02262	0.022	0.51	2333.8		
r(C3)#18	0.0264	0.026	0.51	1973.6		
r(C1)#19	9.739	14.76	0.65	4.4		
r(C2)#19	1	1.46	0.27	18.4		
r(C1)#22	36.79	37.96	0.45	1.2		
r(C3)#22	3.5	29.51	0.3	1.0		
r(C1)#23	4.46	4.49	0.97	21.6		
r(C2)#23	4.99	4.44	0.87	19.6		
r(C3)#23	12.37	9.66	0.96	9.9		
r(C1)#24	8.29	8.42	0.97	11.5		
r(C2)#24	19.38	17.25	0.87	5.1		
r(C3)#24	34.91	29.69	0.96	3.2		
r(C1)#25	7.89	7.56	0.97	12.8		
r(C2)#25	13.76	13.07	0.87	6.7		
r(C3)#25	18.21	16.66	0.96	5.8		

r(C1)#27	2.329	1.32	0.71	54.2		
r(C2)#27	2.5	2.33	0.68	29.1		
r(C3)#27	3.5	4.07	0.87	21.5		
r(C1)#28	7.9	6.59	0.74	11.3		
r(C2)#28	0.011	11.57	0.86	7.4		
r(C3)#28	8.9	6.94	0.95	13.7		
r(C1)#29	35	22.35	0.71	3.2		
r(C2)#29	18.17	18.21	0.66	3.6		
r(C3)#29	8.9	3.64	0.75	20.7		
r(C1)#30	19.1	7.9	0.7	8.9		
r(C2)#30	11.7	11.84	0.6	5.0		
r(C3)#30	7.7	4.97	0.72	14.5		
r(C1)#31	16.5	9.12	0.71	7.8		
r(C2)#31	10.96	10.64	0.66	6.2		
r(C3)#31	8.8	8.5	0.75	8.9		

Speciation plots

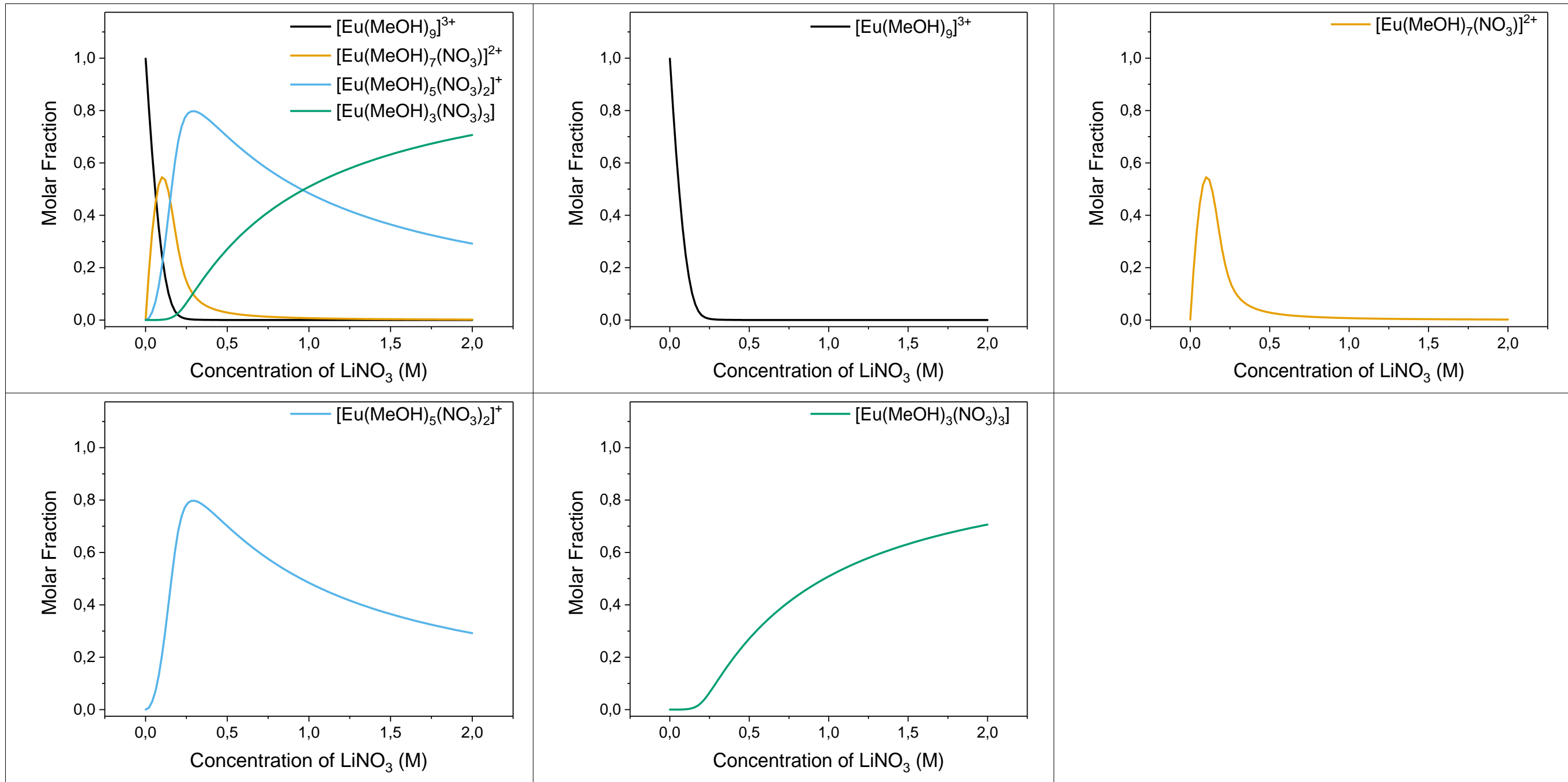


Figure S16: Speciation plots of [Eu(MeOH)₉]³⁺, [Eu(MeOH)₇(NO₃)²⁺], [Eu(MeOH)₅(NO₃)₂]⁺ and [Eu(MeOH)₃(NO₃)₃] as a function of LiNO₃ concentrations made in Dynafit from determined binding constants, see Figure S14 and S15.

Photophysics

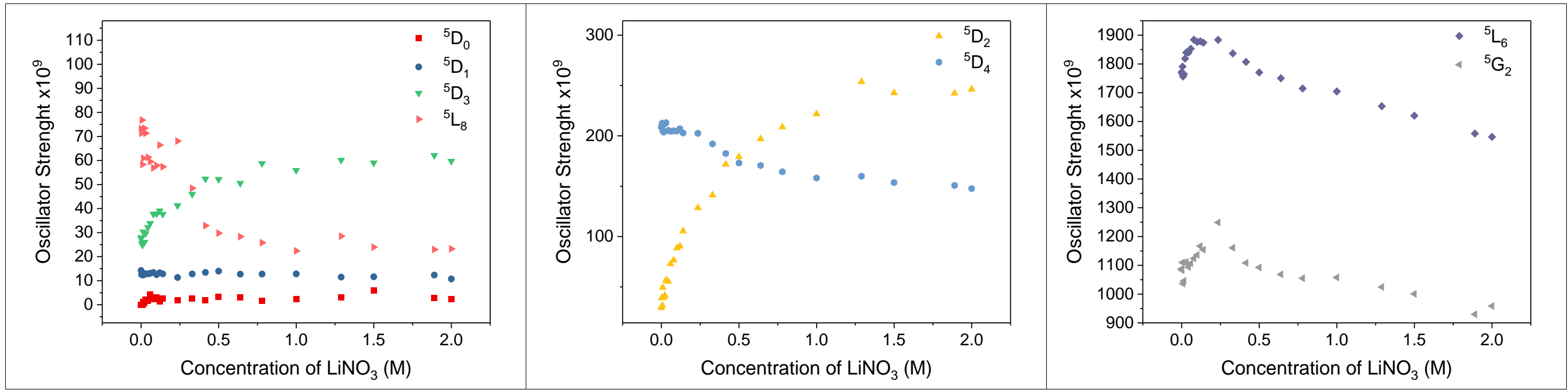
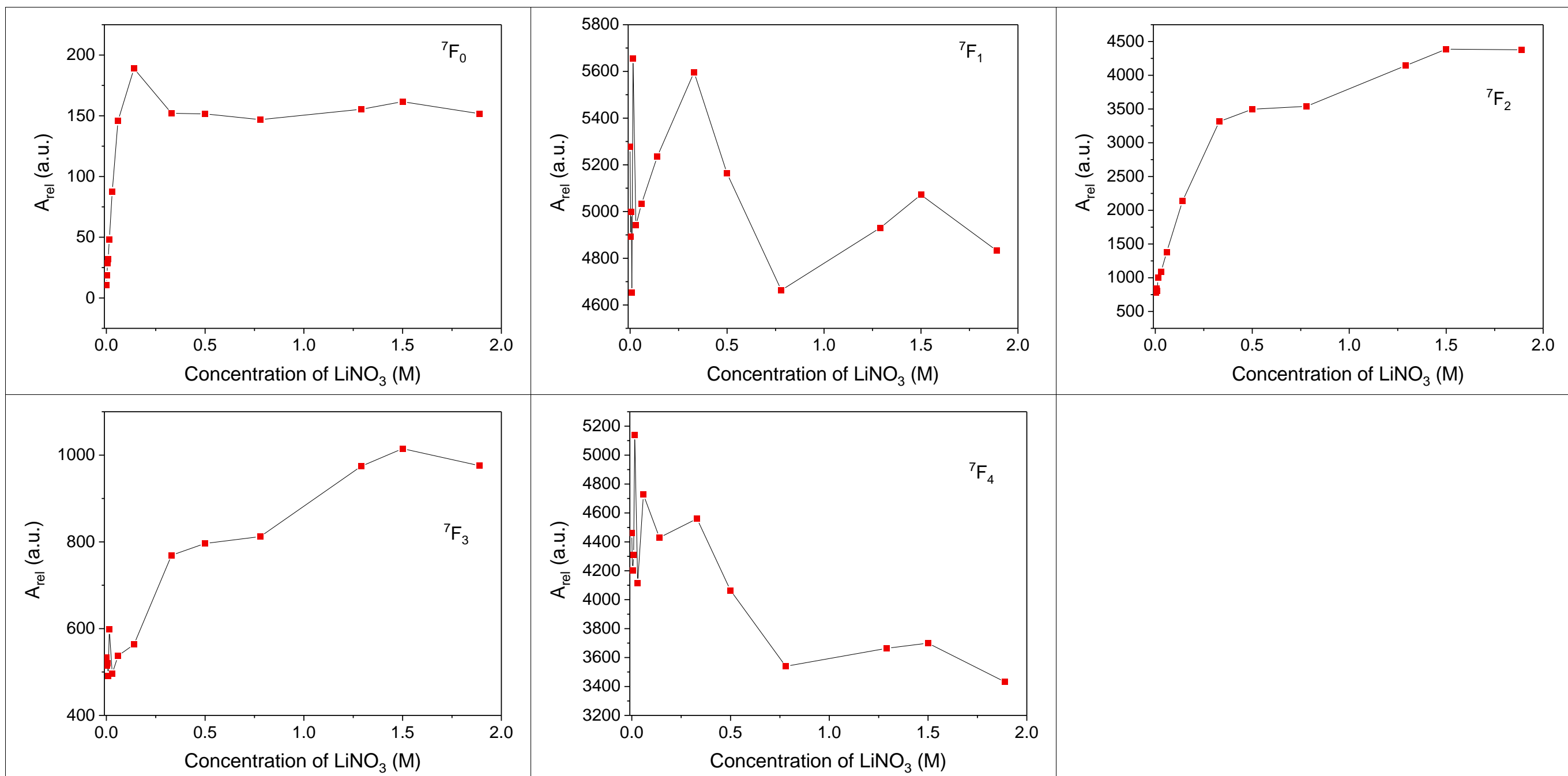


Figure S17: Oscillator strengths of transitions from the ⁷F₀ ground state to the excited state manifold of Eu(CF₃SO₃)₃ in methanol as a function of concentration of LiNO₃. See main text for details

Table S3: Oscillator strengths of transitions from the ⁷F₀ ground state to the excited state manifold of Eu(CF₃SO₃)₃ in methanol as a function of concentration of LiNO₃. See main text for details

[NO ₃ ⁻] (M)	⁵ D ₀	⁵ D ₁	⁵ D ₂	⁵ D ₃	⁵ L ₆	⁵ G ₂	⁵ L ₈	⁵ D ₄
0	0	14	29	28	1772	1088	73	209
0.003	0	13	39	28	1767	1083	71	210
0.006	0	13	31	26	1791	1109	77	213
0.009	0	12	49	25	1756	1036	58	205
0.015	1	12	39	30	1764	1046	61	204
0.0225	1	13	41	26	1819	1110	73	212
0.03	2	13	56	30	1839	1111	71	213
0.0445	2	13	55	32	1840	1093	61	205
0.059	4	13	73	34	1853	1107	60	205
0.0795	2	13	76	38	1884	1124	57	205
0.1	3	12	88	38	1877	1136	58	205
0.12	1	13	90	39	1879	1167	66	207
0.14	2	13	105	38	1874	1154	57	203
0.235	2	11	128	41	1884	1249	68	203
0.33	3	13	141	46	1837	1161	48	192
0.415	2	13	172	52	1807	1108	33	182
0.5	3	14	179	52	1770	1092	30	173
0.64	3	13	197	51	1750	1068	28	171
0.78	2	13	209	59	1715	1055	26	164
1	2	13	222	56	1704	1058	22	158
1.29	3	11	254	60	1653	1025	28	160
1.5	6	12	243	59	1620	1000	24	154
1.89	3	12	242	62	1558	929	23	151
2	2	11	246	60	1546	958	23	148



FigureS18: Relative transition probability (see main text) from the $^5\text{D}_0$ emissive state of $\text{Eu}(\text{CF}_3\text{SO}_3)_3$ to the $^7\text{F}_J$ manifold in methanol as a function of LiNO_3

TableS4: Relative transition probability (see main text) from the $^5\text{D}_0$ emissive state of $\text{Eu}(\text{CF}_3\text{SO}_3)_3$ to the $^7\text{F}_J$ manifold in methanol as a function of LiNO_3

$[\text{NO}_3^-]$ (M)	$^7\text{F}_0$	$^7\text{F}_1$	$^7\text{F}_2$	$^7\text{F}_3$	$^7\text{F}_4$
0	10	5277	782	534	4461
0.003	19	4892	784	515	4203
0.006	29	4998	843	520	4201
0.009	32	4652	809	491	4311
0.015	48	5655	998	598	5140
0.03	88	4940	1088	496	4114
0.059	146	5033	1379	537	4727
0.14	189	5235	2134	563	4429
0.33	152	5597	3314	769	4560
0.5	152	5163	3497	796	4064
0.78	147	4663	3539	812	3539
1.29	155	4930	4141	974	3663
1.5	162	5072	4387	1015	3700
1.89	152	4833	4379	976	3430

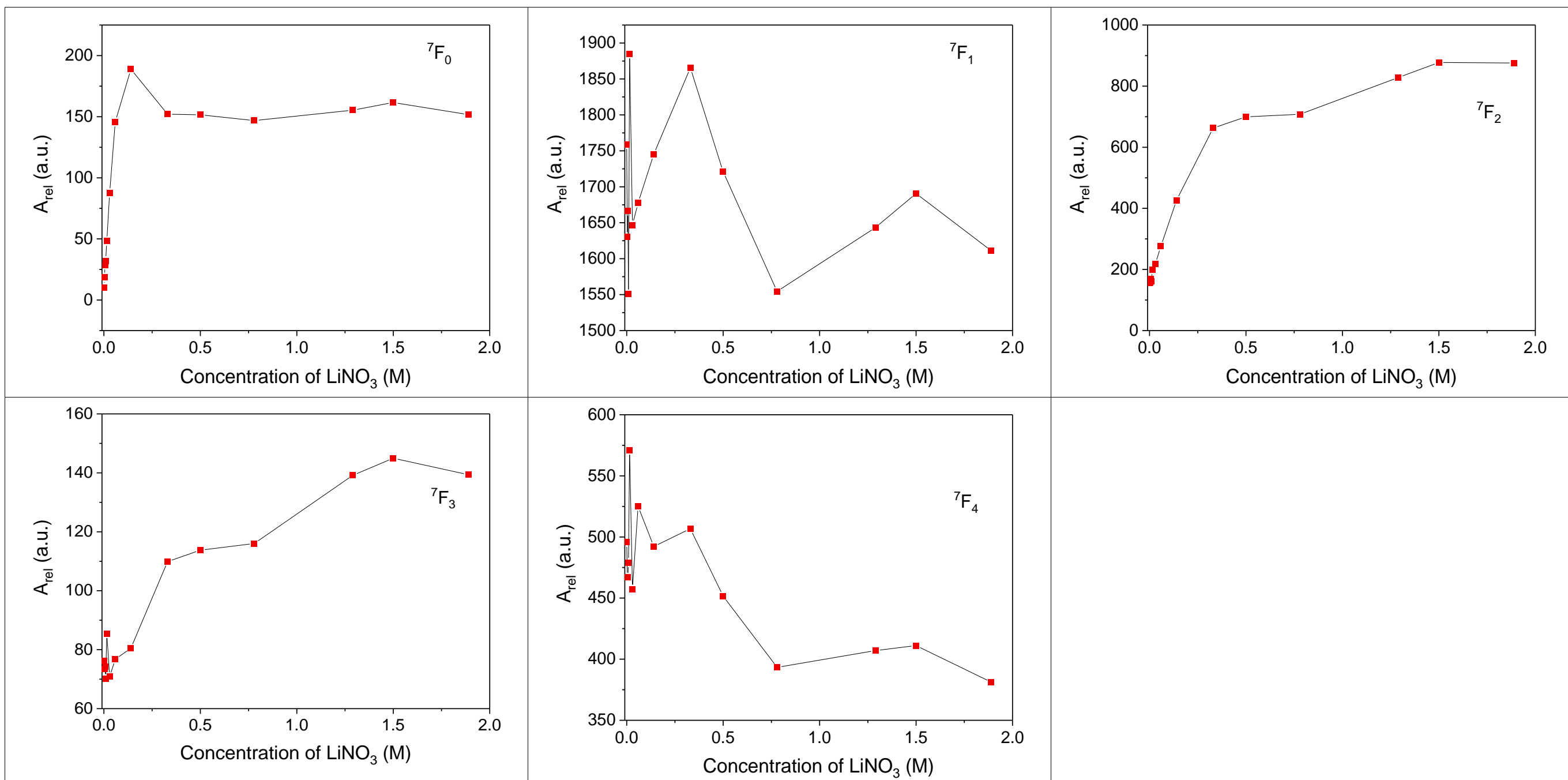


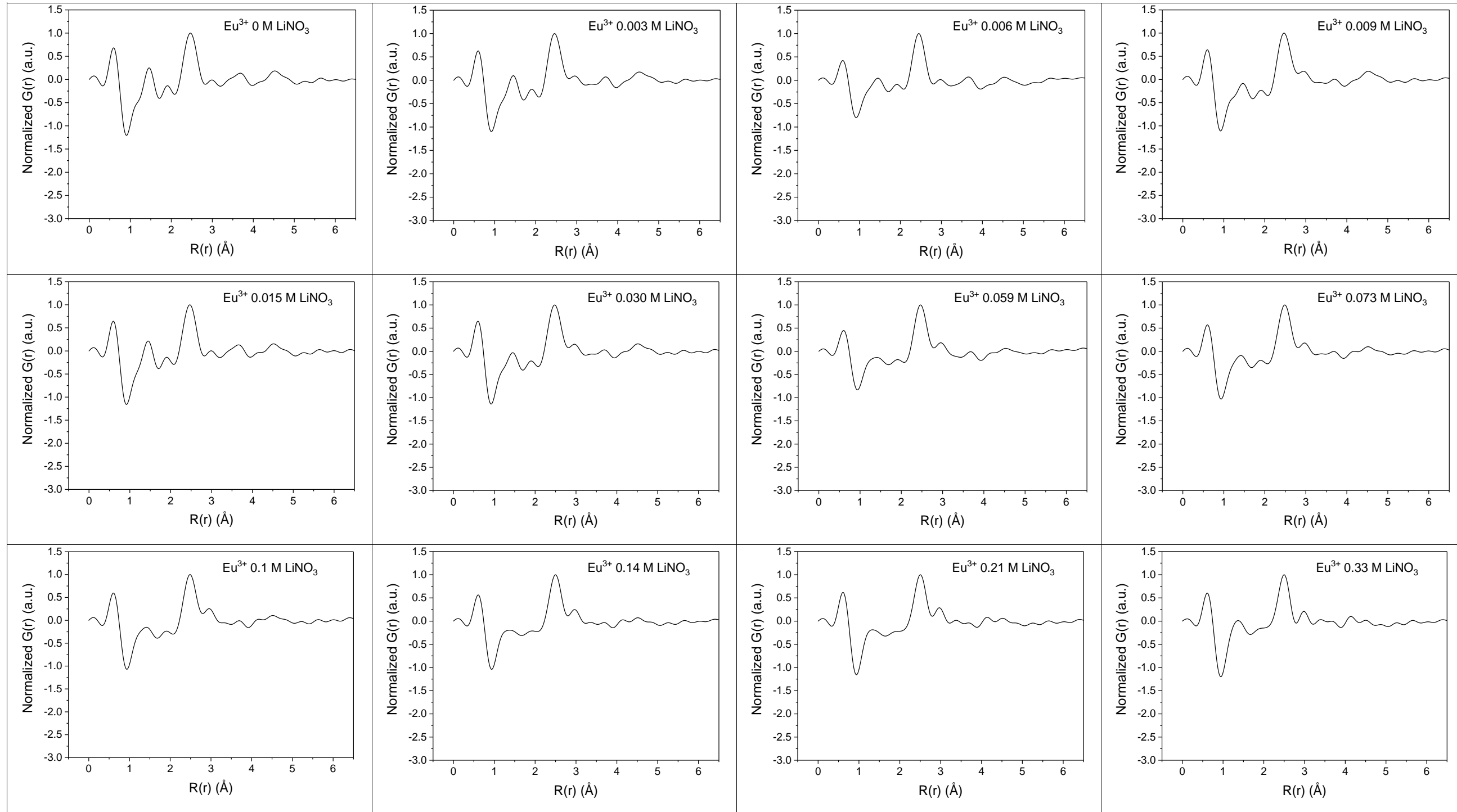
Figure S19: Relative transition probability (see main text) from the $^5\text{D}_0$ emissive state of $\text{Eu}(\text{CF}_3\text{SO}_3)_3$ to the $^7\text{F}_j$ manifold, divided by the total number of microstates in the band, in methanol as a function of LiNO_3 .

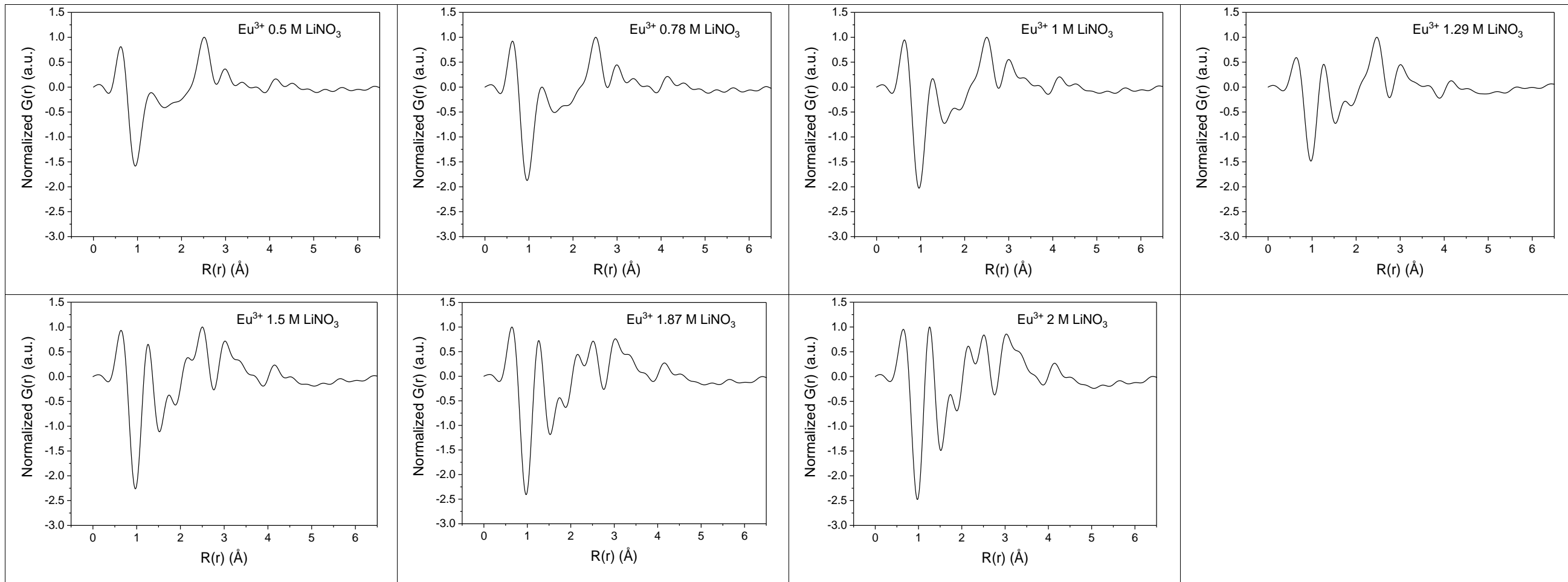
Table S5: Relative transition probability (see main text) from the $^5\text{D}_0$ emissive state of $\text{Eu}(\text{CF}_3\text{SO}_3)_3$ to the $^7\text{F}_j$ manifold, divided by the total number of microstates in the band, in methanol as a function of LiNO_3

A_{rel}	$^7\text{F}_0$	$^7\text{F}_1$	$^7\text{F}_2$	$^7\text{F}_3$	$^7\text{F}_4$
0	10	1759	156	76	496
0.003	19	1631	157	74	467
0.006	29	1666	169	74	467
0.009	32	1551	162	70	479
0.015	48	1885	200	85	571
0.03	88	1647	218	71	457
0.059	146	1678	276	77	525
0.14	189	1745	427	80	492
0.33	152	1866	663	110	507
0.5	152	1721	699	114	452
0.78	147	1554	708	116	393
1.29	155	1643	828	139	407
1.5	162	1691	877	145	411
1.89	152	1611	876	139	381

X-ray Total Scattering

Normalized G(r)





FigureS20: Normalized $G(r)$ of $\text{Eu}(\text{CF}_3\text{SO}_3)_3$ in MeOH with concentrations of LiNO_3 from 0 to 2M.

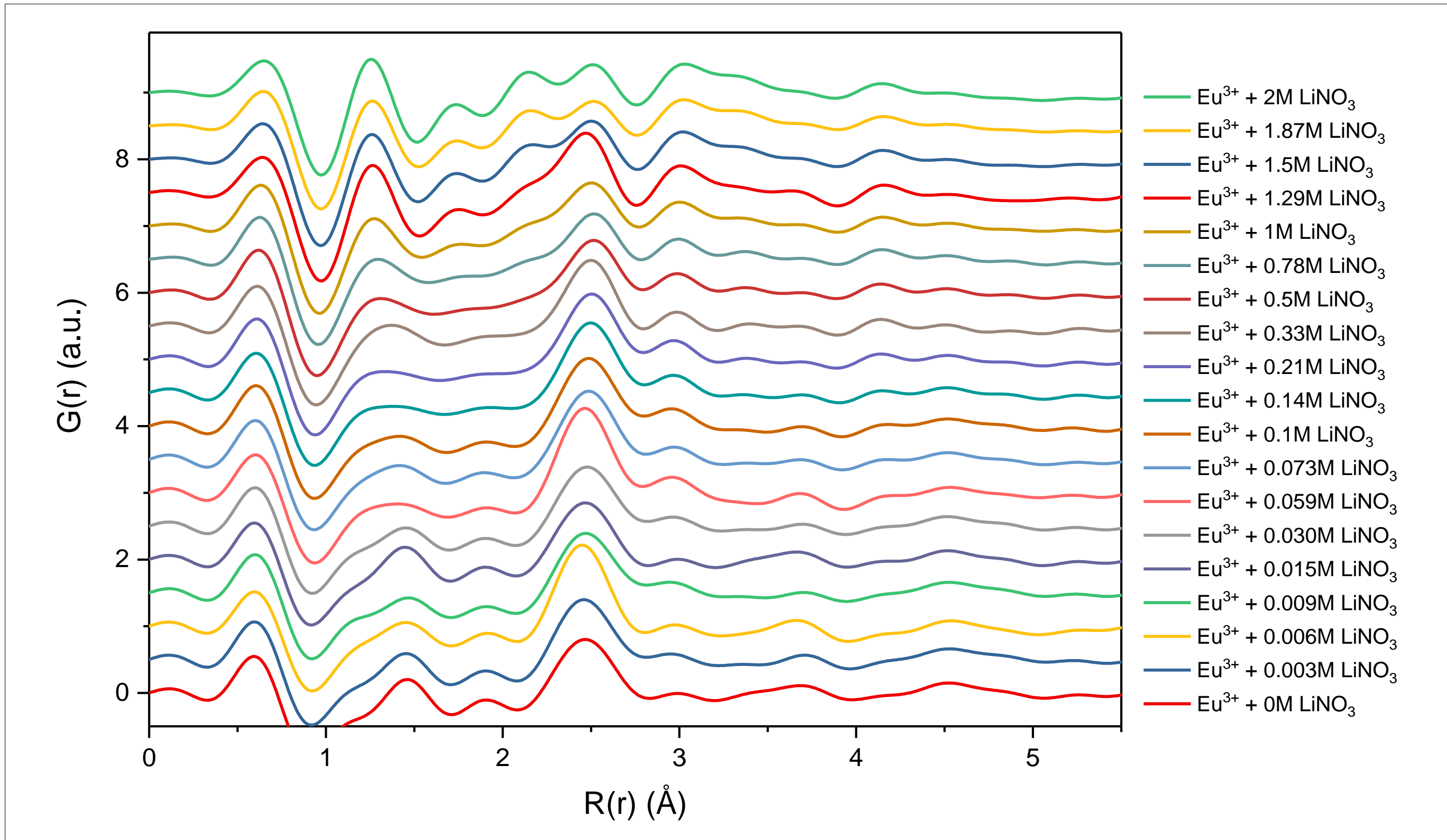
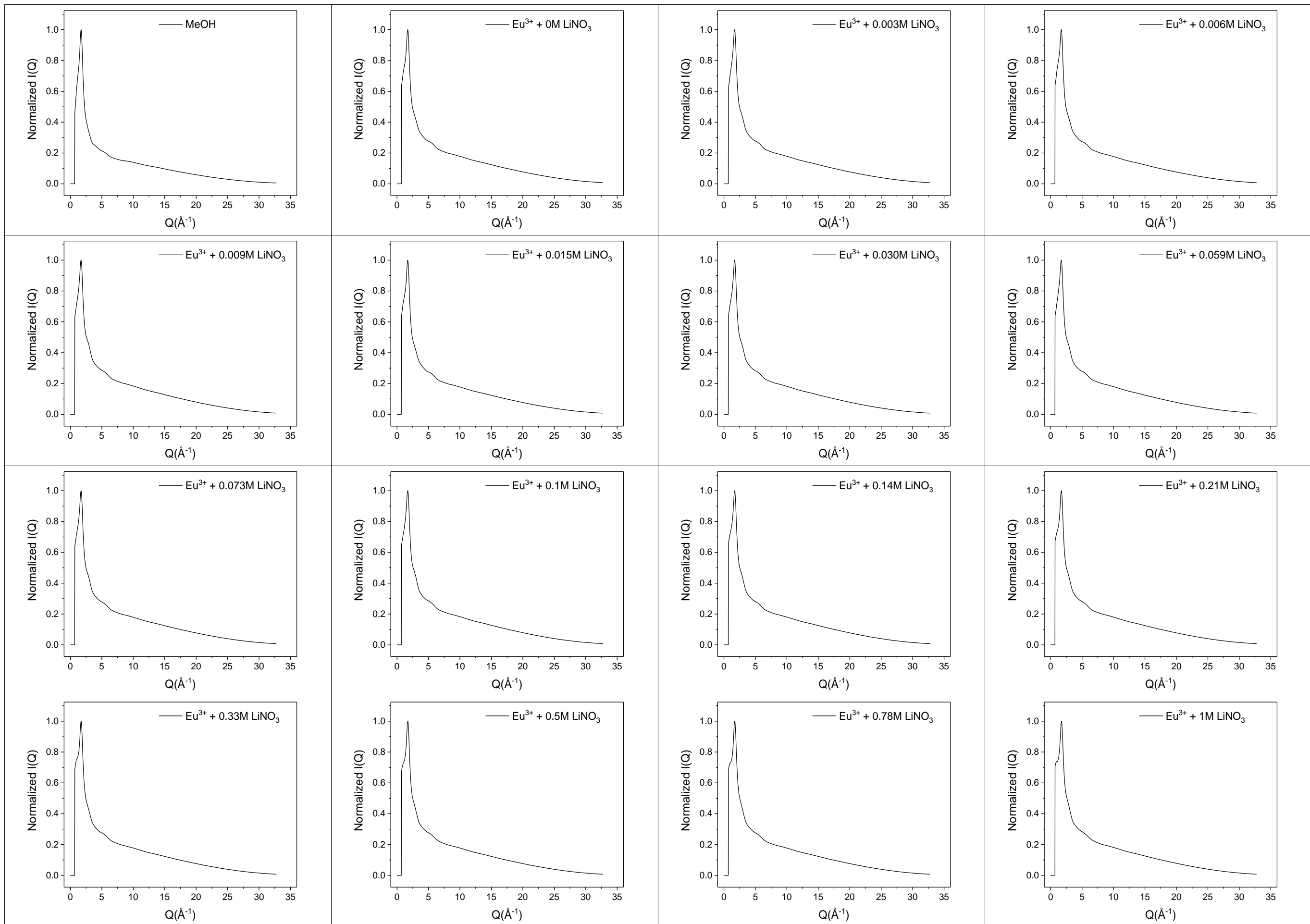


Figure S21: Normalized $G(r)$ of $\text{Eu}(\text{CF}_3\text{SO}_3)_3$ in MeOH with concentrations of LiNO_3 from 0 to 2M.

Normalized I(Q)

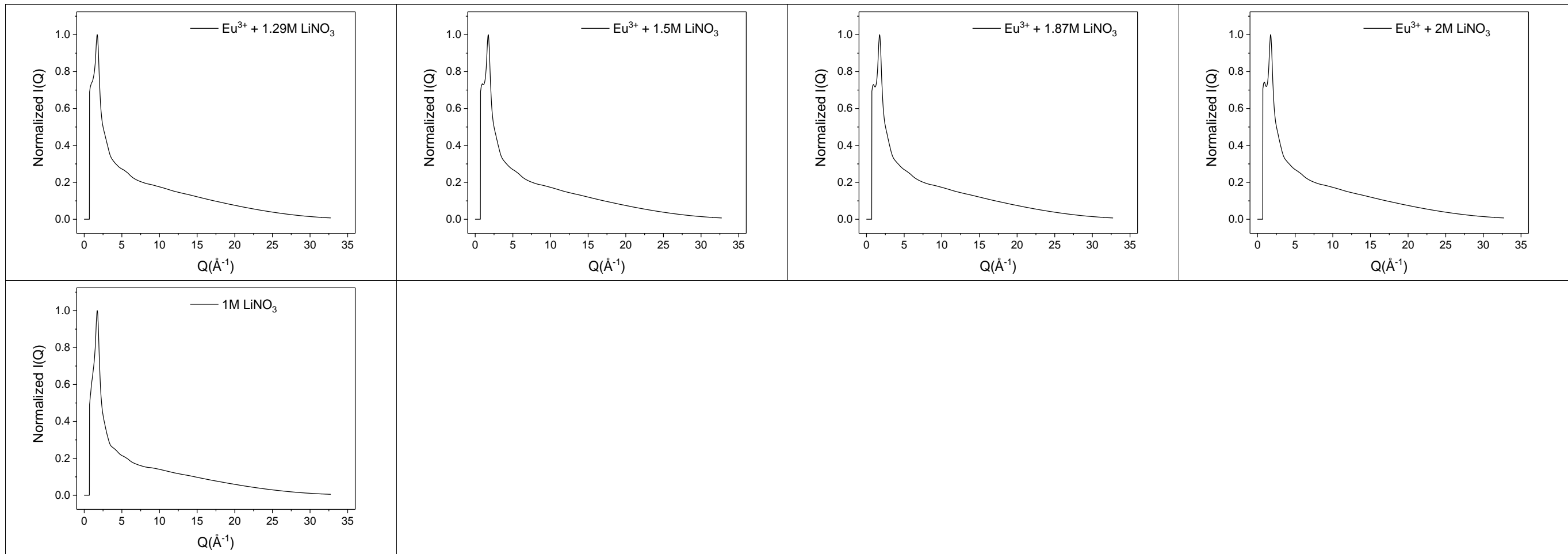
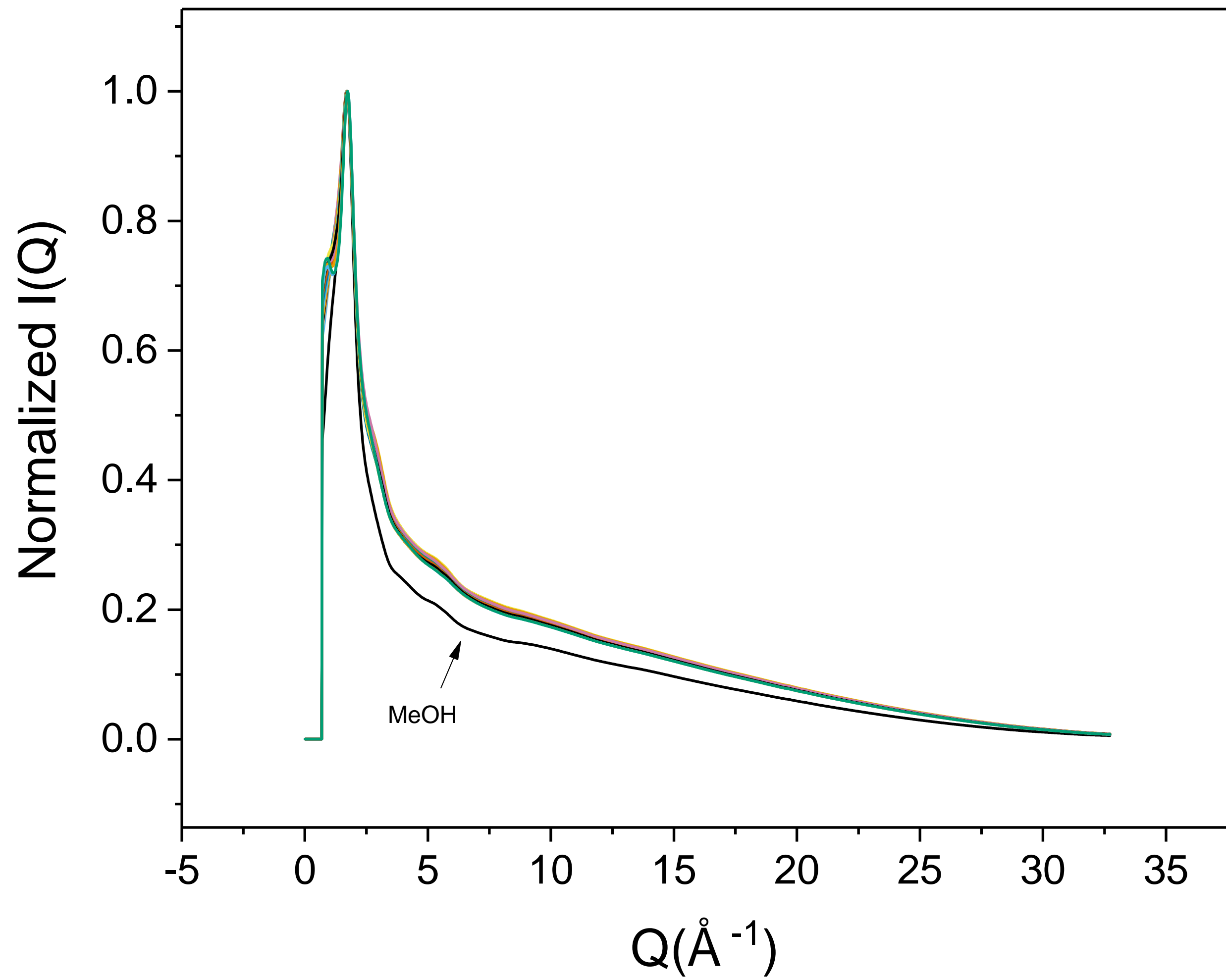
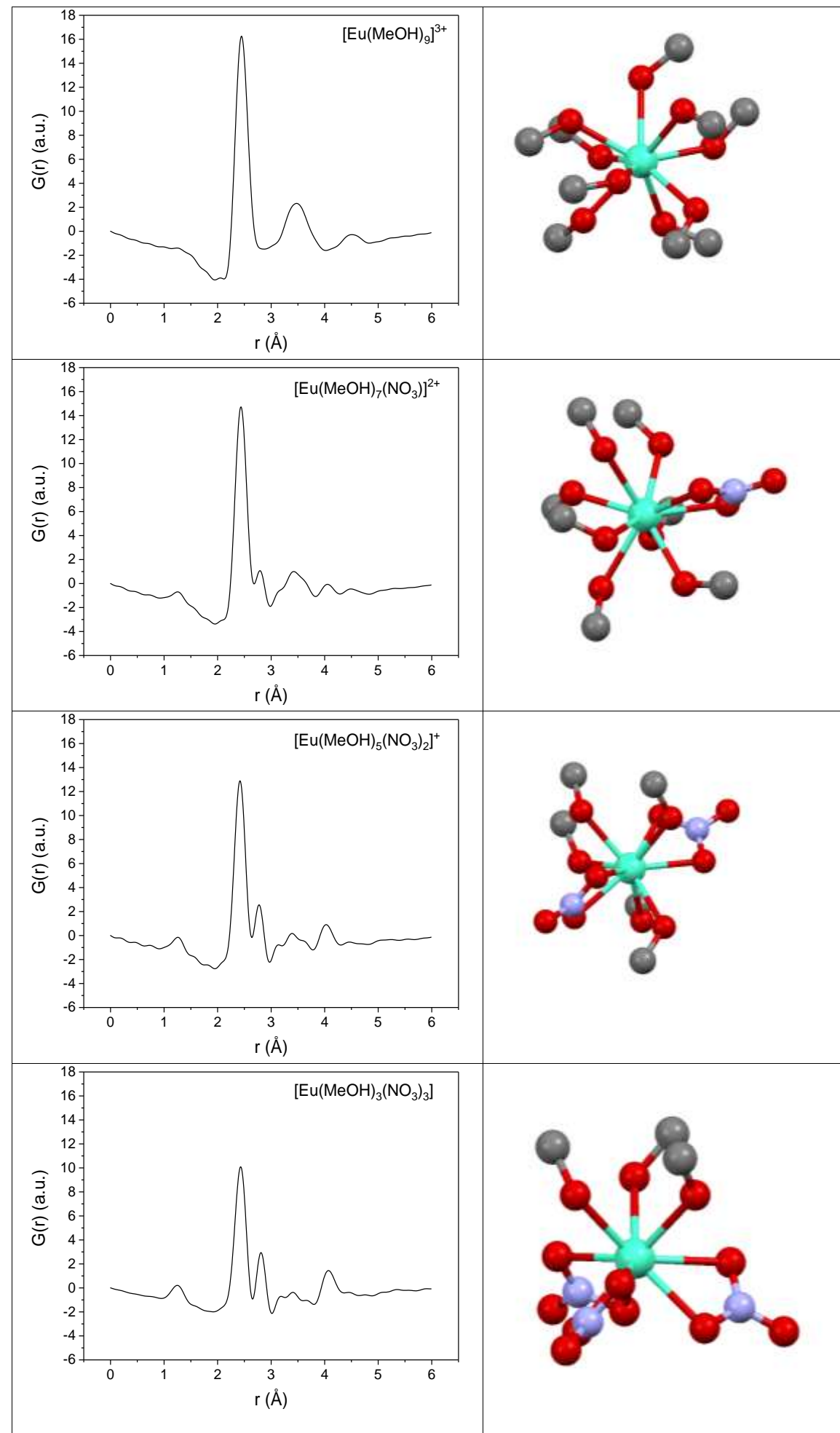


Figure S22: Normalized $I(Q)$ of $\text{Eu}(\text{CF}_3\text{SO}_3)_3$ in MeOH with concentrations of LiNO_3 from 0 to 2M. Background sample of pure MeOH and sample of 1M LiNO_3 in MeOH also shown for comparison

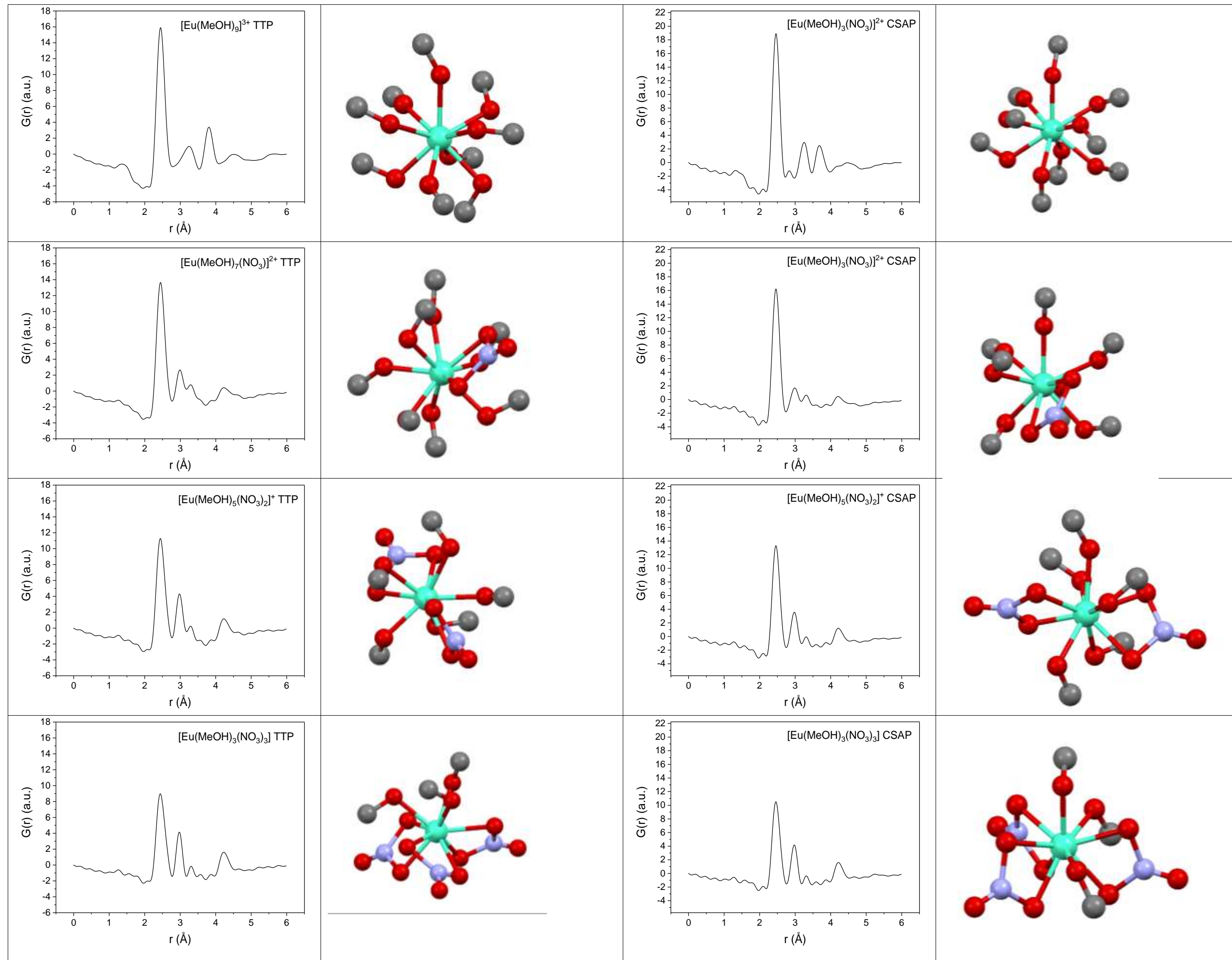


FigureS23: Normalized $I(Q)$ of $\text{Eu}(\text{CF}_3\text{SO}_3)_3$ in MeOH with concentrations of LiNO_3 from 0 to 2M. Background sample of pure MeOH also shown for comparison

Models, Solid state based


FigureS24: Structure and simulated PDF of zero, one, two and three coordinated Eu^{3+} nitrate in methanol. The models were based on the $[\text{Eu}(\text{H}_2\text{O})_9](\text{CF}_3\text{SO}_3)_3$ (CCDC: BUVXAR11)⁴. Hydrogens omitted for clarity

Models, Geometrical



FigureS25: Structure and simulated PDF of zero, one, two and three coordinated Eu^{3+} nitrate in methanol. The models were based on the idealized polyhedral of the TTP and CSAP (Drew)⁵. Hydrogens omitted for clarity

References

1. Horrocks, W. D.; Sudnick, D. R., Lanthanide ion probes of structure in biology. Laser-induced luminescence decay constants provide a direct measure of the number of metal-coordinated water molecules. *Journal of the American Chemical Society* **1979**, *101* (2), 334-340.
2. Beeby, A.; Clarkson, I. M.; Dickins, R. S.; Faulkner, S.; Parker, D.; Royle, L.; de Sousa, A. S.; Williams, J. A. G.; Woods, M., Non-radiative deactivation of the excited states of europium, terbium and ytterbium complexes by proximate energy-matched OH, NH and CH oscillators: an improved luminescence method for establishing solution hydration states. *Journal of the Chemical Society, Perkin Transactions 2* **1999**, (3), 493-504.
3. Tropiano, M.; Blackburn, O. A.; Tilney, J. A.; Hill, L. R.; Just Sørensen, T.; Faulkner, S., Exploring the effect of remote substituents and solution structure on the luminescence of three lanthanide complexes. *Journal of Luminescence* **2015**, *167*, 296-304.
4. Chatterjee, A.; Maslen, E. N.; Watson, K. J., The effect of the lanthanoid contraction on the nonaaqualanthanoid(III) tris(trifluoromethanesulfonates). *Acta Crystallographica Section B* **1988**, *44* (4), 381-386.
5. Drew, M. G., Structures of high coordination complexes. *Coordination Chemistry Reviews* **1977**, *24* (2-3), 179-275.